



ELSEVIER

Contents lists available at ScienceDirect

## Plant Physiology and Biochemistry

journal homepage: [www.elsevier.com/locate/plaphy](http://www.elsevier.com/locate/plaphy)

## Research article

# Comparative transcriptome analysis of *Rosa chinensis* ‘Slater's crimson China’ provides insights into the crucial factors and signaling pathways in heat stress response

Ze Qing Li<sup>a</sup>, Wen Xing<sup>a,\*</sup>, Ping Luo<sup>b</sup>, Fang Jing Zhang<sup>a</sup>, Xiao Ling Jin<sup>a</sup>, Min Huan Zhang<sup>a</sup><sup>a</sup> College of Landscape Architecture, Central South University of Forestry and Technology, Changsha, 410004, Hunan, China<sup>b</sup> Zhejiang Agriculture and Forestry University, Hangzhou, 311300, Zhejiang, China

## ARTICLE INFO

## Keywords:

Heat stress  
Comparative transcriptome analysis  
Co-expression network  
Heat-responsive regulator  
Signaling pathway  
Rose

## ABSTRACT

Heat stress limits the growth of roses and adversely affects the yield and the quality of the rose cut-flowers. To investigate the heat stress response (HSR) mechanisms of rose, we compared the transcriptome profiling generated from *Rosa chinensis* ‘Slater's crimson China’ exposed to heat stress for five different time duration (0, 0.5, 2, 6, 12 h). Overall, 6175 differentially expressed genes (DEGs) were identified and exhibited different temporal expression patterns. Up-regulated genes related to chaperone-mediated protein folding, signal transduction and ROS scavenging were rapidly induced after 0.5–2 h of heat treatment, which provides evidence for the early adjustments of heat stress response in *R. chinensis*. While the down-regulated genes related to light reaction, sucrose biosynthesis, starch biosynthesis and cell wall biosynthesis were identified after as short as 6 h of heat stress, which indicated the ongoing negative effects on the physiology of *R. chinensis*. Using weighted gene co-expression network analysis, we found that different heat stress stages could be delineated by several modules. Based on integrating the transcription factors with upstream enriched DNA motifs of co-expressed genes in these modules, the gene regulation networks were predicted and several regulators of HSR were identified. Of particular importance was the discovery of the module associated with rapid sensing and signal transduction, in which numerous co-expressed genes related to chaperones, Ca<sup>2+</sup> signaling pathways and transcription factors were identified. The results of this study provided an important resource for further dissecting the role of candidate genes governing the transcriptional regulatory network of HSR in Rose.

## 1. Introduction

Roses (*Rosa* spp.) are the important crop in the floriculture industry, and cut roses accounted for an important proportion in the world flower auction market. The optimum temperature for growth and flowering of rose was between 22 and 26 °C. High temperatures restrict the application of roses in the landscape and cut flowers production. Under heat stress conditions, the growth and development of rose was generally limited, and many varieties would enter dormancy directly and do not blossom (Jiang et al., 2009). Therefore, it is imperative to explore the heat stress response mechanism in roses, which is so far limitedly understood.

The molecular mechanisms of HSR and thermo-tolerance have been deciphered in model plants, such as *Arabidopsis thaliana* (Suzuki et al., 2011; Baron et al., 2012; Ohama et al., 2016) and *Solanum lycopersicum* (Baniwal et al., 2004; Frank et al., 2009). It has been demonstrated that

different genes and pathways were regulated by the short-term and long-term heat stress. More chaperones, heat-responsive transcriptional regulators and genes involved in signal transduction were typically stimulated by the short-term heat stress (Qin et al., 2008; Mangelsen et al., 2011; Ohama et al., 2017). Whilst multiple molecular chaperones, crucial transcriptional regulators and key components of signaling pathways triggered by early heat stress are found to be often interconnected in the HS response and finally enhance thermo-tolerance by activation of the expression of HS-regulated genes (Baniwal et al., 2004; Kotak et al., 2007; Nagamangala et al., 2010). Molecular chaperones well known to be involved in early HSR are heat shock protein genes (HSPs), which are very important in preserving protein stability under heat stress (Baniwal et al., 2004); while several members of heat shock transcription factors family (HSFs) serving as the central transcriptional regulators play a crucial role in signaling pathways and are involved in regulating the expression of downstream genes including HSPs

\* Corresponding author.

E-mail address: [Xingw426@sina.com](mailto:Xingw426@sina.com) (W. Xing).<https://doi.org/10.1016/j.plaphy.2019.07.002>

Received 8 January 2019; Received in revised form 30 June 2019; Accepted 1 July 2019

Available online 02 July 2019

0981-9428/ © 2019 Published by Elsevier Masson SAS.

(Koskull-döring et al., 2007a,b). In addition, in *Arabidopsis thaliana*, calmodulin, abscisic acid (ABA), ethylene (ET) and inositol-3-phosphate (IP3) are all known to participate in signal transduction of heat stress and induce the activation of various downstream sensors and kinases, which are involved in acquired thermo-tolerance (Mittler et al., 2004; Dobrá et al., 2015; Ohama et al., 2017). However, the crucial HS-responsive genes and the signal transduction pathways under heat stress in rose have not yet been investigated. To date, except *RcHSP17.8* gene encoding cytosolic class I small heat shock protein (Jiang et al., 2009), no other gene associated with the HSR has been reported.

With the development of next-generation RNA sequencing and genome sequencing, comparative transcriptome studies are successfully used to investigate the signaling pathways and gene networks of HSR in non-model plant species. A series of heat stress-responsive genes and several signal regulation pathways were identified in *Chrysanthemum ankingense* (Sun et al., 2014), *Dianthus caryophyllus* (Wan et al., 2015) and *Rhododendron hainanense* (Zhao et al., 2018), which provides many interesting gene candidates for genetic engineering to reduce negative effects on the growth of plants. Using transcriptome sequencing, Pei et al. (2013) identified ethylene-responsive transcripts in modern rose petals. Recently, the genome sequence of *R. chinensis* ‘Old Blush’ was released (Raymond et al., 2018), providing a valuable database for further functional and genomic research in rose. However, to date, no transcriptome studies has been performed to investigate the early events of HSRs in rose.

*R. chinensis* ‘Slater's crimson China’, the diploid species of *Rosa*, is one of the most important species that participated in the *R. hybrida* breeding. It may represent a convenient genomic model for cultivars, and harbor potentially beneficial genes. In the present study, in order to detect initial molecular changes in response to short-term heat stress, and comprehensively identify the crucial genes involved in signal transduction pathways, we compared the transcriptome profiling of *R. chinensis* ‘Slater's crimson China’ exposed to heat stress for five different time durations (0, 0.5, 2, 6 and 12 h). Combined with physicochemical and transcriptomic data, the major heat responsive processes in *R. chinensis* could be summarized, and a series of gene candidates that can improve early HSR without negatively effects were identified. This study enhances our understanding about the HSR in *R. chinensis* at the molecular level and may also provide a useful molecular biology reference for further studies on other *R. hybrida* cultivars and *Rosa* species.

## 2. Materials and methods

### 2.1. Plant materials and treatments

2-year-old healthy cutting seedlings of *R. chinensis* were grown at Changsha city of Hunan Province, central south China. The plant material was planted in the pot with an inner size of 20 cm in diameter and 22 cm in height, containing a soil mixture of peat and perlite (2:1). The size and height of plant materials employed in all experiments were almost the same. Before high temperature treatment, the samples were cultured in the artificial climate chambers at 25/25 °C day/night temperature, 12 h/12 h (day/night) photoperiod with a light intensity of  $200 \mu\text{mol m}^{-2} \text{s}^{-1}$  and 70% relative humidity for 40 days. Subsequently, these samples were subjected to constant 42 °C HS for 0 h (control), 0.5 h, 2 h, 6 h, 12 h, 18 h and 24 h in the same artificial climate chamber with a light intensity of  $200 \mu\text{mol m}^{-2} \text{s}^{-1}$  and 70% relative humidity. Each treatment group contained three replicates. For physiological measurement, the fourth or fifth fully expanded leaves from 3 replicates were harvested at 0, 2, 6, 12, 18 and 24 h after heat treatment, respectively. For RNA-seq, leaves from 3 replicates treated under heat stress for 0, 0.5, 2, 6 and 12 h were collected for RNA isolation and sequencing, respectively. Leaves collected from five treatment groups for gene expression analysis were immediately frozen in liquid nitrogen and stored at  $-80 \text{ °C}$  until required for further analyzing.

### 2.2. Measurement of chlorophyll fluorescence parameters

The fourth or fifth fully expanded leaves from 3 replicates in each treatment were used for chlorophyll *a* fluorescence transients measurements. Chlorophyll fluorescence parameters, including maximal photochemical efficiency of PSII (Fv/Fm), apparent electron transport rate (ETR), non-photochemical quenching (NPQ) and fluorescence in the light ratio (Fv'/Fm'), were measured in vivo using the LICOR 6400 system (LICOR Biosciences, Inc. Lincoln, NE) and calculated as described by Song et al. (2014). Prior to the measurement of Fv/Fm and NPQ, the leaves were adapted to dark in the LI-6400XT leaf chamber for 20 min.

### 2.3. Measurement of physiological and biochemical parameters

The total superoxide dismutase (SOD) activity was determined using the spectrophotometer by measuring its ability to inhibit the photochemical reduction of nitro blue tetrazolium (NBT), according to Chen et al. (2011). Malondialdehyde (MDA) as the index of membrane lipid peroxidation was measured by 10% (w/v) trichloroacetic acid (TCA) reaction using the absorption photometry method at 450, 532, and 600 nm, as described by Duan et al. (2005). Soluble sugars were analyzed using the phenol-sulfuric acid method described by Wang et al. (2014).

### 2.4. RNA extraction, cDNA library construction, and illumina sequencing

Total RNA was extracted from the leaves treated with heat-stress for 0 h, 0.5 h, 2 h, 6 h and 12 h in triplicate, as previously described by Xing et al. (2014). Electrophoresis on 1% agarose gel was performed and the Agilent 2100 RNA 6000 Kit was used to test the integrity and purity of RNA. mRNA was purified from the total RNA using oligo (dT) beads and was used for library preparation. Fifteen cDNA libraries were constructed from the mRNA of three independent biological samples of five treatments (0, 0.5, 2, 6, and 12 h) as previously described by Yan et al. (2016), and sequenced on the Illumina HiSeq™ Xten platform at the Wuhan Igenebook Biotechnology Co., Ltd., Wuhan, China ([www.igenebook.com](http://www.igenebook.com)).

### 2.5. De novo assembly and function annotation

The clean reads were filtered from the raw reads by removing primer and adaptor sequences, raw reads with ambiguous bases ‘N’ (N > 10%), as well as low quality reads (more than 50% Q ≤ 5). Then, the clean reads were assembled into contigs using Trinity de novo software (Grabherr et al., 2011). Tgicl v2.0.6 was used to clustered contigs to unigenes (Pertea et al., 2003). ESTScan (v3.0.3, default parameters) was used to predict the putative protein translations (Iseliet al.1999).

All the unigenes were aligned with sequences in NCBI non-redundant database (Nr) (<http://www.ncbi.nlm.nih.gov/>), NCBI non-redundant nucleotide sequences database (NT), Swiss-Prot database (<http://www.expasy.ch/sprot/>) and eukaryotic Ortholog Groups database (KOG) (<http://www.ncbi.nlm.nih.gov/cog/>) by NCBI blast 2.2.28+ (E value <  $1.0 \text{ E}^{-5}$ ). The cut-off E-value of the Nr, Nt and Swiss-Prot databases was  $10^{-5}$ , while the KOG database was  $10^{-3}$ . To further annotate all unigenes, we use the Blast2GO program and the WEGO software for GO annotations and GO functional classification with the e-value threshold of  $1.0 \text{ E}^{-6}$  (Ye et al., 2006). In addition, we matched all unigenes with the KEGG pathway database to predict pathway that unigenes participate in by BLASTx (E value <  $1.0 \text{ E}^{-5}$ ).

### 2.6. Identification of differentially expressed genes (DEGs)

The expression level of each Unigreen was calculated by the RPKM (reads per kilo base per million clean reads) method as previously

described by Shi et al. (2017). All read counts were normalized to RPKM value, representing gene expression level. DESeq2 package (1.10.1) was used to perform the differential expression analysis. Using the negative binomial distribution methods and the Benjamini-Hochberg methods, differentially expressed genes (DEGs) were identified with a false discovery rate (FDR) < 0.001. For further analyses, we used an additional criterion, which involved using only differentially expressed genes (DEGs) with the  $|\log_2(\text{fold change})| \geq 1$  change in expression as screening criteria. Fold change (FC) represents the ratio of the expression of the two treatments. Besides, GO functional enrichment and KEGG pathway enrichment analysis of DEGs were conducted by the Goseq R package with hypergeometric distribution algorithms and KOBAS with Fisher's exact test as previously described by Shi et al. (2017) (Bonferroni-corrected  $p$ -value  $\leq 0.05$ ).

### 2.7. Co-expression network analysis

Weighted Gene Co-expression Network Analysis (WGCNA) was performed to conduct the gene co-expression network, as previously described by Langfelder and Horvath (2008). The modules were generated using the block wise Modules function with the power of 16, the min Module Size of 30, and the merge Cut Height of 0.2. Then, GO and KEGG enrichment analyses were conducted for genes in each module ( $P$ -value < 0.05). Moreover, hub genes were selected from all of the selected modules (> 200 edges).

### 2.8. Motif enrichment analysis and the prediction of transcriptional regulatory network

We followed the approach described by Garg et al. (2017) to predict the potential DNA motifs and their associated transcription factors (TFs) in modules with some modifications. Firstly, we mapped all the genes in each module back to the released reference genome. Then we analyzed 2-kb upstream sequences of these genes and identified significantly enriched DNA sequence motif using HOMER. Further, the TFs binding with these potential binding motifs in the same modules were identified using AGRIS database and the gene ontology enrichment analysis for the co-expression genes harboring these potential binding motifs was performed using clusterprofiler. The GO terms exhibiting a corrected  $P$ -value of < 0.05 were considered to be significantly enriched. The predicted regulatory network of GO terms of target genes, DNA motifs and their associated TFs were visualized via Cytoscape.

### 2.9. Real-time quantitative RT-PCR validation

Eighteen DEGs were chosen randomly to validate gene expression profile data using Real-time quantitative RT-PCR (RT-qPCR) method. RT-qPCR was carried out on 7500 Fast Real-Time PCR System (Applied Biosystems) as previously described by Xing et al. (2014). The RNA samples used in the DGE experiments were used for qRT-PCR assays. All reactions were performed in triplicate for technical replicates and biological replicates of three individuals. Gene-specific primers of the selected Unigreen sequences (Table S18) were designed using Primer Premier 5.0 software. The *RhGAPDH* (Glyceraldehyde-3-phosphate dehydrogenase) gene was used as the internal standard in each reaction.

### 2.10. Statistical analysis

Data of physiological responses were analyzed using ANOVA, and means were compared using the least significant difference (LSD) at  $P = 0.05$ . All computations were made using the SAS statistical analysis package.

## 3. Results

### 3.1. High-throughput transcriptome sequencing and read assembly

The main characteristics of the fifteen cDNA libraries, created from three independent biological samples of five treatments (0, 0.5, 2, 6, and 12 h), were summarized in Table S1. After removal of adaptor sequences, ambiguous nucleotides and low-quality sequences, ~39,133,888 to ~69,319,324 clean reads of fifteen libraries were obtained. The Q20 and Q30 values (sequencing error rate < 1%) were more than 99% and 96%, respectively. The G + C percentages were more than 45%. Using Trinity software, these clean reads were assembled into 440,071 contigs with a total length of 548,936,260bp. The length of the contigs ranged from 201 to 19,674bp, with an average size of 1247.4bp. The N50 was 2,316bp, and N90 was 482bp (Additional file 1: Table S2). A total of 95,099 contigs were longer than 2 kbp. More than 88% of the reads could be mapped back to the assembled contigs (Additional file 1: Table S3). Fifteen transcriptomic data have been deposited to NCBI's Sequence Read Archive (SRA) under the accession number SRP150297.

### 3.2. Gene expression under the different heat stress stages

Differentiation of gene expression at 42 °C for four different time duration (0.5, 2, 6 and 12 h) was analyzed in comparison to the control grown at 24 °C. The number of DEGs increased from 0.5 h to 12 h, and reached a peak at 0 h vs. 12 h comparison set, illustrating that most of the heat regulated genes are late-response. 1202 (32.9%) genes were identified exclusively at 12 h of heat treatment, while only 106 (2.9%), 381 (10.4%) and 238 (6.5%) genes were specific at 0.5, 2 or 6 h of heat treatment. 3655 differentially expressed genes (DEGs) were identified on at least one time during HS treatment; while 276 DEGs were obtained at all four different time duration (Fig. 1A).

Meanwhile, analysis of DEGs revealed that the number of up-regulated genes between CK and 2 h is the largest among the four stages, while the number of down-regulated genes at this stage is the smallest, suggesting many important genes participated in the early HSR were up-regulated in this period (Fig. 1B). In addition, a total of 3400 DEGs (1466 up-regulated and 1934 down-regulated) were detected between HS\_0.5 h and HS\_12 h, which is the largest of all. While, only 252 (9 up-regulated and 143 down-regulated) DEGs were detected between HS\_6 h and HS\_12 h, which is the smallest of all (Fig. 1B).

On the one hand, a heat map was generated to characterize the global clustering and expression pattern of the significantly regulated genes during heat stress treatments. As shown in Fig. 2, DEGs can be divided into three major expression patterns of response. Type I included genes that were significantly up-regulated at all four time points, and exhibited highest expression level at 0.5–2 h, while type II included genes that were up-regulated at 6–12 h of heat stress. Genes in type III were down-regulated from 0.5 h to 12 h of heat stress. In addition, according to the hierarchical cluster analysis, a large proportion of DEGs followed a similar expression pattern in 0 h and 0.5 h, as well as 6 h and 12 h of heat treatment, which clustered together, while the expression profile of 2 h heat treatment clustered separately (Fig. 2). These data may indicate that the gene expression patterns during the early phases of heat stress were different from that during the late phases, and 2 h was the major switch in the global gene expression patterns, at which some crucial genes inducing the expression of heat response genes during the regulation of heat signaling are expressed.

### 3.3. GO functional enrichment and KEGG pathway enrichment analysis of DEGs

According to GO functional enrichment analysis, 168, 189, 167 and 212 terms for the up-regulated DEGs were enriched in 0 h vs. 0.5 h, 0 h vs. 2 h, 0 h vs. 6 h and 0 h vs. 12 h, respectively. The most significantly

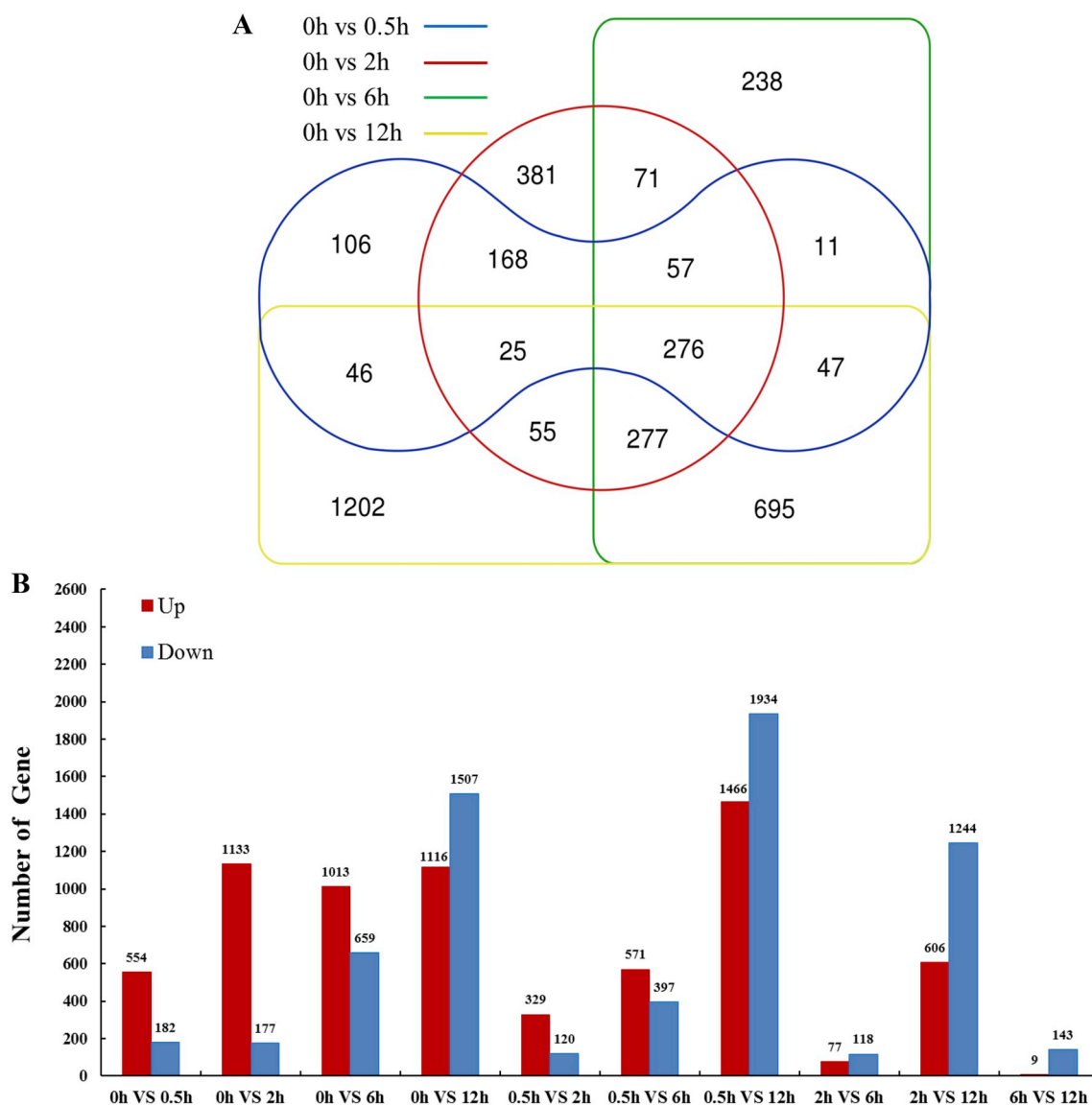


**Fig. 1.** Changes in gene expression profile among the different heat stress stages. (A) Venn diagram analysis of the number of the differentially expressed genes (DEGs) at the four heat stress treatment time points compared with control plants. (B) The number of up-regulated and down-regulated genes between two different heat stress treatment time points. The vertical axis reflects the numbers of up-regulated and down-regulated genes. Up- and down-regulated genes are shown red and blue bars, respectively. (For interpretation of the references to color in this figure legend, the reader is referred to the Web version of this article.)

overrepresented terms of GO terms for the up-regulated DEGs in 0 h vs. 0.5 h and 0 h vs. 2 h focused on the defense and protective steps respond to the stress, including seven terms in the category of biological processes, which were ‘protein folding (GO: 0006457)’, ‘response to stress (GO: 0006950)’, ‘response to stimulus (GO: 0050896)’, ‘unfolded protein binding (GO: 0051082)’, ‘response to temperature stimulus (GO: 0009266)’, ‘response to inorganic substance (GO: 0010035)’. The significantly enriched GO terms for the up-regulated DEGs at 6 h heat treatment were similar to those at 12 h. Most of the top 10 enriched terms in 0 h vs. 6 h and 0 h vs. 12 h were involved in ribosome and cytosolic ribosome, including the cellular components category (ribosome, GO: 0005840; ribonucleoprotein complex, GO: 0030529; cytosolic ribosome, GO: 0022626), the biological processes category (ribosome biogenesis, GO: 0042254; ribonucleoprotein complex biogenesis, GO: 0022613) and the molecular function category (structural constituent of ribosome, GO: 0003735) (Additional file 2: Table S4). Additionally, 74, 46, 245 and 426 terms for down-regulated DEGs were enriched in 0 h vs. 0.5 h, 0 h vs. 2 h, 0 h vs. 6 h and 0 h vs. 12 h, respectively. The down-regulated genes showed a very different picture.

In samples with heat treatment for 0.5 h, 16 of the top 20 enriched GO terms for the down-regulated DEGs belonged to the biological processes category such as cell wall organization, RNA biosynthetic process and transcription, suggesting the repression of biological processes upon heat stress at this time point; while in samples with heat treatment for 2 h, the top 20 enriched GO terms for the down-regulated DEGs were similar to those for 6 h and 12 h. The most significantly overrepresented terms focused on thylakoid, plastid, chloroplast, membrane and extra-cellular region within cellular components category (Additional file 2: Table S5), which indicated that the negative effect on the metabolic activity of these cellular compartments occurred as short as 2 h of heat stress treatment.

The KEGG pathway analysis demonstrated the existence of two phases during the heat stress treatment period. The pathways enriched for 0 h vs 0.5 h and 0 h vs 2 h DEGs were similar (Additional file 3, Table S6). Among the top 10 enriched pathways, chaperones and folding catalysts (ko03110), protein processing in endoplasmic reticulum (ko04141), transporters (ko02000), MAPK signaling pathway (ko04010) and protein phosphatase and associated proteins (ko01009)

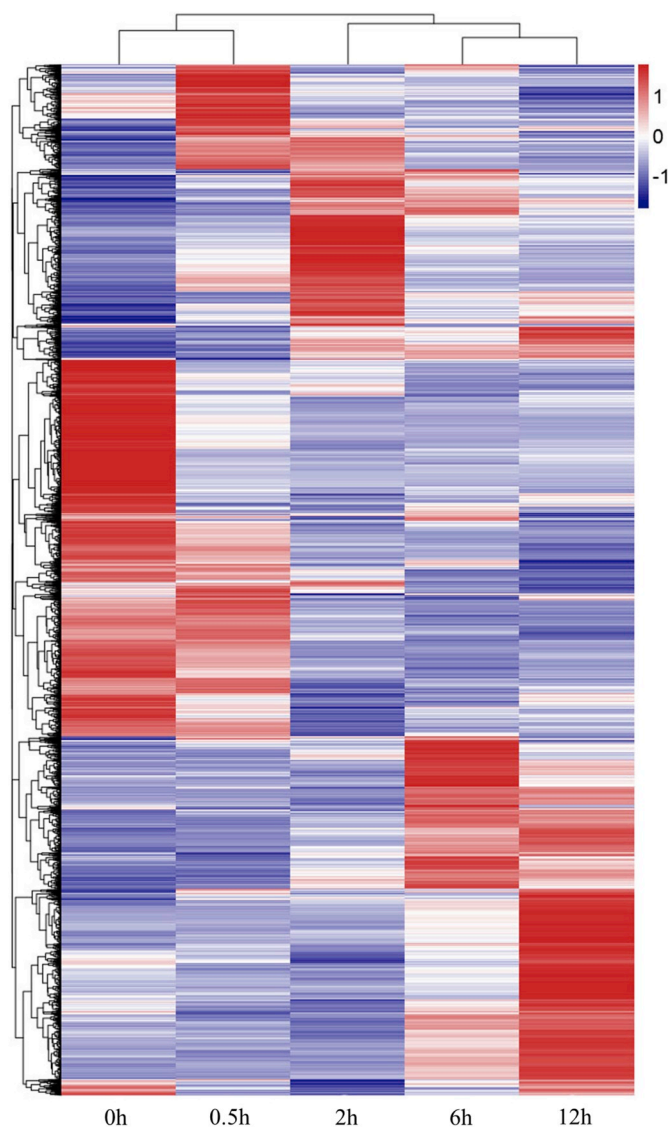


**Fig. 2.** The heat-map of the total differentially expressed genes (DEGs). Columns and rows in the heat maps represent samples and genes, respectively. Color scale indicates the values of  $\log(\text{RPKM} + 1)$ . Color from red to blue, indicated that the  $\log_{10}(\text{RPKM} + 1)$  values were from small to large, blue color indicates high expression level and red color indicates low expression level. (For interpretation of the references to color in this figure legend, the reader is referred to the Web version of this article.)

were regulated in response to 0.5–2 h heat stress. Moreover, glutathione metabolism (ko00480) and ascorbate and aldarate metabolism (ko00053) were enriched in 0 h vs 0.5 h. These results indicated that heat stress had been sensed and signaling transduction pathways had been activated after 0.5–2 h of heat stress treatment. However, after 6 h of heat treatments, many more pathways linked with metabolism were enriched, especially those associated with photosynthesis. Among the top 10 enriched pathways, photosynthesis proteins (ko00194), porphyrin and chlorophyll metabolism (ko00860) and polyketide biosynthesis proteins (ko01008) were enriched in 0 h vs 6 h; flavonoid biosynthesis (ko00941) and proline metabolism (ko00330) were enriched in 0 h vs 12 h. While photosynthesis - antenna proteins (ko00196), photosynthesis (ko00195) and carbon fixation in photosynthetic organisms (ko00710) were enriched in 0 h vs 6 h and 0 h vs 12 h (Additional file 3, Table S6). These results indicated that these metabolism processes may act as the predominant processes of the HSR in *R. chinensis* after 6 h of heat treatment.

### 3.4. Signal transduction pathways response to heat stress in *R. chinensis*

In this study, 68 genes annotated as protein kinases and phosphatases involved in signal transduction were identified in *R. chinensis* (Additional file 6, Table S10). 26 of them were up-regulated in 0.5 h and 2 h heat treatment samples. Five genes related to G-type lectin S-receptor-like serine/threonine-protein kinase were found to show the highest degree of upregulation. Additionally, twenty five DEGs encoding the components of the  $\text{Ca}^{2+}$ /calmodulin-mediated signal network were induced during 0.5–12 h of heat stress, including annexin, calcium-binding proteins (CBPs), calcium-dependent protein kinases (CDPKs),  $\text{Ca}^{2+}$ -binding protein EF hand, calmodulin (CaM) and CaM-related proteins. Ten of these  $\text{Ca}^{2+}$  signaling-related genes were up-regulated by heat stress, and eight of them were up-regulated by 2.64- to 7.72-fold in 0 h vs 0.5 h. Among them, contig\_66454 (CDPK), contig\_67665 (Calmodulin binding protein) and contig\_89966 ( $\text{Ca}^{2+}$ -binding protein EF hand) were up-regulated 7.72-, 6.16- and 4.81-fold, respectively (Fig. 4, Additional file 6, Table S11).

Moreover, for genes detected at 0.5–2 h, the KEGG pathway involved in ‘MAPK signaling pathway (ko04010)’ was significantly enriched in this study, and 5 DEGs were highly similar to MAPK genes, including MAPKKK1 (MEKK1), MAPKKK (ANP1), MAPKKK (YODA) and MAPK3 (MPK3). One gene (contig\_42393) encoding MAPKKK (ANP1) was up-regulated during the 0.5 h and 2 h heat treatment; one gene (contig\_31359) encoding MAPKKK (YODA) was up-regulated only at 2 h<sub>HS</sub>; and one gene (contig\_10784) encoding MAPKKK1 (MEKK1) was down-regulated during all the heat treatment. Two genes encoding MAPK3 were down-regulated at 12 h<sub>HS</sub> (Additional file 6, Table S10).

### 3.5. Heat shock proteins (HSPs) and other chaperones were highly activated by heat stress

The ‘protein processing in endoplasmic reticulum’ (ko04141) and ‘Chaperones and folding catalysts’ (ko03110) pathways existed in the top 10 enriched pathways at all four time points of heat stress treatment. 96 HSPs were significantly expressed in response to heat stress, of which 94 were up-regulated and 2 were down-regulated, with  $\text{Log}_2\text{FC}$  values ranging from  $-2.76$  to  $12.07$  (Additional file 4, Table S7). Among these HS-induced HSPs, 69 were highly induced at all four time points; 11 had an elevated expression level at 0.5–6 h. The expression level of these HSP genes were sharply increased at HS\_0.5 h, and then reached its peak at HS\_2 h, but decreased to relatively low levels after the 6–12 h heat treatment (Additional file 4, Table S7), which were, however still significantly higher than that in the control samples. Whilst 11 HSPs were only up-regulated at 0.5 h–2 h; only 3 HSPs were induced after 6 or 12 h treatment. In detail, these HS-induced HSPs belonged to four major classes of HSP families, including 26 small HSPs (HSP20, HSP18.1, HSP18.5, HSP17.8 and HSP15.7), 48 HSP70 and 19 HSP90 and 2 HSP101. We also observed that all small HSPs (sHSPs) were significantly up-regulated ( $\text{Log}_2\text{FC} \geq 5$  on at least one time point) under heat treatment, and most of these sHSPs were located in mitochondrial, chloroplast and cytosolic. Among these, the expression of HSP17.8 and HSP101 increased by approximately 11.3-fold and 8.7-fold in the 2 h heat treatment, respectively.

In addition to HSP, 21 genes belonging to peptidyl prolyl cis-trans isomerase family were highly induced by heat stress in this study, among which 16 genes were up-regulated (see Additional file 4, Table S8). Ten ROF1-encoding genes were elevated for more than five-fold from 0.5 h heat treatment, while two FKBP15-1-encoding, one FKBP42-encoding, and two CYP18-1-encoding genes were induced for more than three-fold from 2 h heat treatment.

### 3.6. Transcription factors responding to heat stress in *R. chinensis*

We performed a thorough search for transcription-factor of differentially expressed transcripts and identified numerous transcripts

**Table 1**  
Numbers of transcription factors up- and down-regulated in different heat treated samples.

Category	Total		0 h VS 0.5 h			0 h VS 2 h			0 h VS 6 h			0 h VS 12 h			
	up	down	total	up	down	total	up	down	total	up	down	total	up	down	total
AP2/DREB	4	3	7	4	2	6	4	1	5	3	2	5	3	3	6
HSF	12	1	13	7	0	7	11	0	11	6	1	7	6	1	7
WRKY	8	20	28	0	4	4	2	6	8	1	7	8	5	19	24
NAC/NAM	19	3	22	2	1	3	12	0	12	11	1	12	10	2	12
MYB	17	18	35	2	2	4	6	1	7	4	9	13	10	17	27
AP2/ERF	8	25	33	0	14	14	4	6	10	5	9	14	3	23	26
C2H2	3	4	7	1	1	2	1	2	3	2	3	5	0	4	4
bHLH	6	8	14	1	1	2	2	1	3	3	2	5	4	7	11

including up- and down-regulated genes belonging to different transcription factor (TF) families (Additional file 5, Table S9). The HSF (13), WRKY (28), AP2/DREB (7), AP2/ERF (33), NAC/NAM (22), MYB (35), basic helix–loop–helix (bHLH) (14) and zinc finger protein (23) families were the top nine largest families. Genes in some TF families, such as GRAS, TCP, NFYB, ARF, and TFIIB were also identified from DEGs.

The expression patterns of these transcription factors were complex at four heat treatment stages (Table 1, Fig. 3). Twelve DEGs encoding HSFs, including HSF30, HSF24, HSF45, HSF4a, HSF3, HSF8, HSF2a, and HSF2b exhibited the greater change in expression levels (Fig. 3A, Additional file 5). Expression of eleven HSFs was increased under heat stress, and only one (HSF8) was repressed after 6 h of heat

stress exposure. With regard to expression responses at different HS time points, genes encoding HSF2a, HSF3 and HSF30 were up-regulated at all four time points and showed highest expression level at HS\_2h; gene encoding HSF2b had a significantly elevated expression level at HS\_0.5h and HS\_2h; while genes encoding HSF4a and HSF24 were up-regulated only at HS\_2h. We also found that most HSF genes (ten) showed highest expression level at HS\_2h. Among these HSFs, contig\_245724 (HSF30) and contig\_60744 (HSF2b) showed the highest up-regulation of expression with 7.411 and 6.483-fold, respectively.

Another overrepresented family of upregulated TFs was the NAC family, with 22 members (Fig. 3B, Additional file 5). Among these HS-

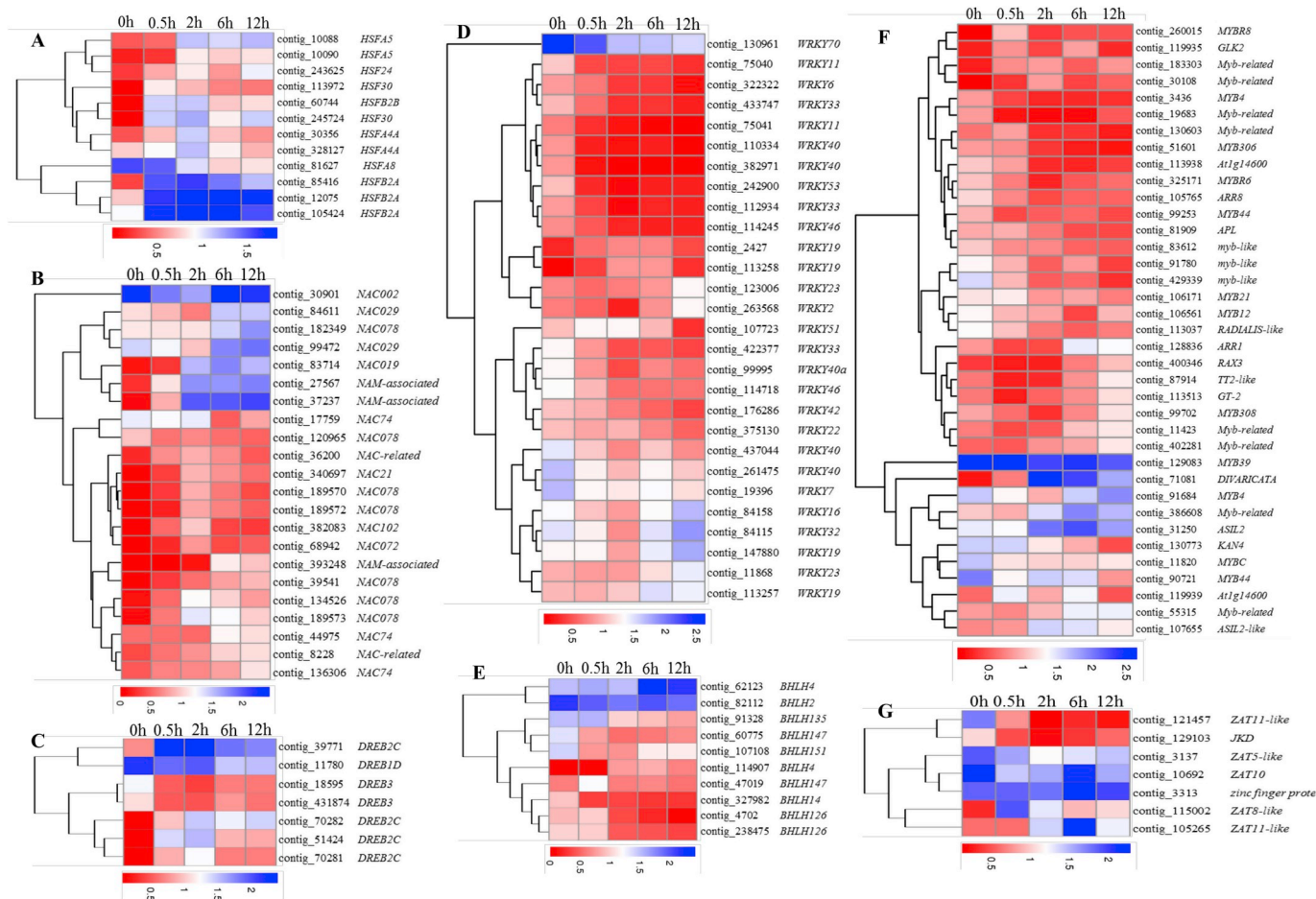


**Fig. 3.** Heat-map of differentially expressed genes involved in different transcription factors. (A) Heat map of HSF genes. (B) Heat map of NAC/NAM genes. (C) Heat map of DREB genes. (D) Heat map of WRKY genes. (E) Heat map of BHLH genes. (F) Heat map of MYB/MYC genes. (G) Heat map of zf-C2H2 genes. Data for the relative expression levels of genes were obtained by DGE data after taking  $\log_{10}(\text{RPKM} + 1)$ . Color from red to blue, indicated that the  $\log_{10}(\text{RPKM} + 1)$  values were from small to large, blue color indicates high expression level and red color indicates low expression level. (For interpretation of the references to color in this figure legend, the reader is referred to the Web version of this article.)

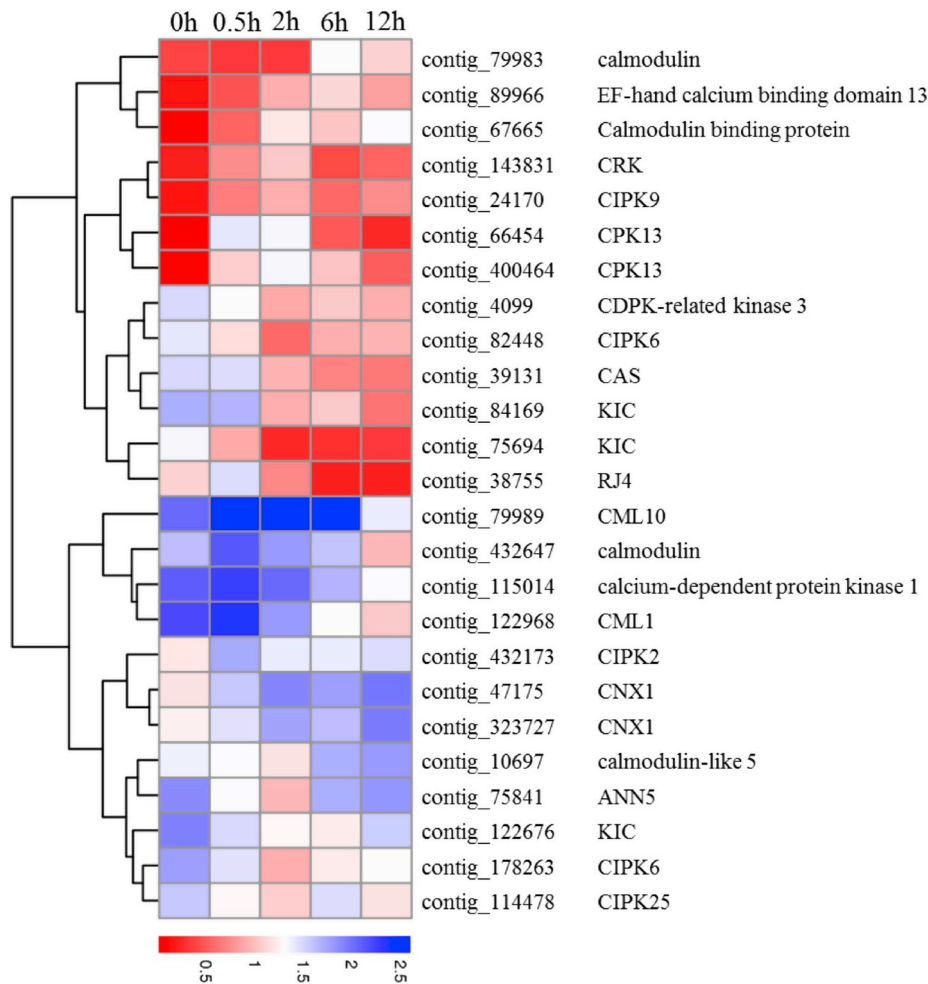


**Fig. 4.** Heat-map of differentially expressed genes involved in Calcium signal. Data for the relative expression levels of genes were obtained by DGE data after taking  $\log_{10}(\text{RPKM} + 1)$ . Color from red to blue, indicated that the  $\log_{10}(\text{RPKM} + 1)$  values were from small to large, blue color indicates high expression level and red color indicates low expression level. (For interpretation of the references to color in this figure legend, the reader is referred to the Web version of this article.)

responsive NACs, 19 were up-regulated, including 11 exhibiting the higher up-regulation of expression for more than 4-fold on at least one time point during HS treatment. While Contig\_382083 (*NAC102*) and contig\_83714 (*NAC019*) were upregulated by 8.87- and 7.13-fold, respectively. In addition, we also found that 2 members of Multiprotein bridging factor (MBF1) were up-regulated more than 4-fold at all four HS time points, and the expression of contig\_38537 similar to *AtMBF1C* was reached 8.18-fold at 2 h heat treatment.

On the contrary, among WRKY, AP2/ERF, bHLH and ARF/AUX/IAA families, more genes were down-regulated under heat treatment. 20 of 28 DEGs similar to *WRKY* were down-regulated under heat stress by 2.17- to 4.48-fold. Expression of contig\_422377 (*WRKY33*) was decreased by 3.91-fold, compared with the control group (Fig. 3D, Additional file 5).

Among MYB, AP2/DREB and C2H2 transcription factors, the up- and down-regulated members were balanced. 35 members of *MYBs* were found to be responsive to heat stress, which was more than all other families. Of these *MYB* genes, 16 were up-regulated during HS, from 1.56- to 9.85-fold (Fig. 3F, Additional file 5). While among seven AP2/DREB transcription factors, four encoding DREB2C exhibited highly dynamic changes ( $\text{Log}_2\text{FC} \geq 6$  on at least one HS time point) and were upregulated early, from around 0.5 h. The expression of contig\_51424 (*DREB2C*) was up-regulated 7.36-fold at 2 h (Fig. 3C, Additional file 5). In addition, 3 of 7 *C2H2* genes were up-regulated during HS (Fig. 3G, Additional file 5).

### 3.7. ROS producing and ROS-scavenging gene response to heat stress in *R. chinensis*

According to GO analysis, the GO term, namely 'response to reactive oxygen species' (GO: 0000302), was significantly enriched at 0.5 h and 2 h HS treatment time points, and 'response to oxidative stress' (GO: 0006979) was significantly induced at 6 h and 12 h HS treatment time points. While the 'antioxidant activity' (GO: 0016209) GO term was enriched at all four HS time points. Thus, ROS formation may be one of the major effects of the early heat stress in *R. chinensis*. Meanwhile, the MDA content and antioxidant enzyme activities measured in this study showed that the MDA concentration has no significant change at the HS\_2 h and HS\_6 h treatment but increased from 12 h heat treatment and peaked at the HS\_24 h treatment (Additional file 13, Fig. S1C); while antioxidant enzyme activities peaked at the HS\_6 h treatment, then gradually decreased from the HS\_12 h to HS\_24 h treatment (Additional file 13, Fig. S1A).

A total of 63 ROS production or scavenging related genes were identified (Additional file 7, Table S12). Among ROS production related genes, ones coding putative respiratory burst oxidase protein, ferric reduction oxidase, peroxisomal (S)-2-hydroxy-acid oxidase, long-chain-alcohol oxidase were all down-regulated at HS\_6 h and HS\_12 h; only gene encoding amine oxidase (contig\_63874) was up-regulated at 0.5 h and 2 h (Additional file 7, Table S12). Additionally, 46 DEGs involved in enzymes with ROS-scavenging activity, including peroxidase (POD),

ascorbate peroxidase (APX), monodehydroascorbate reductase (AFRR), glutathione S-transferase (GST), glutathione peroxidase (GPX), polyphenol oxidase (PPO), ferritin, glutaredoxin, thioredoxin and peroxiredoxin, and some genes encoding SOD, APX, GPX, AFRR, GST, ferritin, glutaredoxin and thioredoxin were up-regulated on at least one of the treatment times. Among these genes encoding antioxidant enzymes, *APX1* (contig\_877994) was up-regulated by 6.61-fold at HS\_0.5 h, but decreased to control level from 2 h to 12 h; and gene encoding Ferritin-3 (contig\_114325) was up-regulated at 0.5 h and 2 h, but decreased to control level at 12 h. Moreover, of 11 genes encoding GST, four (contig\_65049, contig\_407695, contig\_65048 and contig\_393868) were found to be up-regulated at all four HS time points, and showed the most significant responses to the HS\_2 h treatment ( $\text{Log}_2\text{FC} \geq 5$ ); Three (contig\_96995, contig\_97000, contig\_392027) were up-regulated from HS\_2 h treatment; and two were (contig\_140582, contig\_246816) induced at 6 h and 12 h heat treatment. Moreover, two genes (contig\_143266, contig\_99201) encoding thioredoxin-like protein also showed significant responses to all of the four HS time points, and reached the expression level at HS\_2 h ( $\text{Log}_2\text{FC} \geq 5$ ) (Additional file 7, Table S12).

### 3.8. Involvement of photosynthesis-related genes in heat stress response

Through GO analysis, we observed that three GO terms, namely 'Photosynthetic membrane' (GO: 0034357), 'photosynthesis' (GO: 0015979) and 'chloroplast thylakoid membrane' (GO: 0009535), were the overrepresented in DEGs down-regulated after heat stress treatment of 6 h–12 h (Additional file 2, Table S5), and numerous genes involved in photosynthesis significantly declined during 6 h–12 h heat stress treatment.

In all, 48 DEGs involved in the light reactions were identified in this study. Among them, 9 DEGs encoded the components of PSI, including 2 up-regulated genes (*PsaA*, *CAB8*) and 7 down-regulated genes (Fig. 5A, C). 24 DEGs were detected for PSII, including 2 up-regulated genes (*PsbP*, *PsbY*) and 22 down-regulated genes (Fig. 5A, C). In addition, we also observed 15 genes for the redox chain: two genes encoding PGR5 (PROTON GRADIENT REGULATION) were significantly up-regulated after heat stress treatment of 12 h, while 13 genes encoding Cytochrome *b6-f* complex, Cytochrome *c*-type biogenesis *ccda*-like, F-type ATP synthase, photosynthetic NDH subunit of subcomplex, Blue copper protein and ferredoxin–NADP reductase were down-regulated (Fig. 5A, D). Most of these genes declined significantly during 6–12 h heat treatment, suggesting that PSII and PSI was inhibited and electron transfer in photosynthesis might suffer negative effects under heat stress at this period. To confirm this result, we measured the maximum quantum efficiency of PSII ( $F_v/F_m$ ), fluorescence in the light ratio ( $F_v'/F_m'$ ), apparent electron transport rate (ETR), and non-photochemical quenching (NPQ) (Fig. 6). Compared with the control group,  $F_v/F_m$ ,  $F_v'/F_m'$  and ETR were not significantly changed after heat stress treatment of 2 h, but decreased from HS\_6 h to HS\_24 h. While NPQ decreased significantly and constantly.

Meanwhile, in the category of energy metabolism, 'Carbon fixation in photosynthetic organisms' (ko00710) was also significantly enriched during heat stress treatment of 0.5–12 h (Additional file 3, Table S6). A total of 42 DEGs involved in photosynthetic CO<sub>2</sub> fixation were identified, including 18 and 24 genes up-regulated and down-regulated, respectively (Additional file 8, Table S13). Among these genes, 12 genes encoding phosphoribulokinase, RuBisCO large subunit-binding protein subunit alpha, triosephosphate isomerase, phosphoenolpyruvate carboxylase, ribulose-phosphate 3-epimerase and ribose-5-phosphate isomerase were significantly up-regulated with more than 5-fold change (Fig. 5B, E, F). Moreover, among 16 DEGs involved in photorespiration, only 3 genes encoding Ribulose biphosphate carboxylase/oxygenase activase (RCA), ribulose-phosphate 3-epimerase and GTP-binding protein were up-regulated under heat stress treatment; the other genes, including *PGLP1B* (PHOSPHOGLYCOLATE PHOSPHATASE 1B), *HAOX1*

(Peroxisomal (S)-2-hydroxy-acid oxidase) and *ybdL* (Aminotransferase *ybdL*) were repressed (Fig. 5B, E, F, Additional file 8, Table S13).

In addition, the expression of 11 genes encoding chlorophyll synthesis and one gene encoding plastoquinone biosynthesis were significantly decreased, including Magnesium-chelatase subunit *chlI* (*CHLI*), protochlorophyllide reductase (*POR*), Coproporphyrinogen-III oxidase (*CPX*), glutaminyl tRNA synthetase (*HEMA*), et (Additional file 8, Table S13).

### 3.9. Involvement of carbohydrate metabolism and transport in heat stress response of *R. chinensis*

A total of 97 DEGs involved in carbohydrate metabolism were identified in our experiment, most of which are involved in sucrose glucose, hexose, monosaccharide, pectin, alcohol, mannose, cellular polysaccharide metabolic, biosynthetic and catabolic processes (Additional file 9, Table S14).

Among these genes, except genes encoding bidirectional sugar transporter, most genes related to carbohydrate transport, such as sugar carrier protein, glucose-6-phosphate/phosphate translocator, sugar transport protein, hexose transporter, glycerol-3-phosphate transporter and inositol transporter, were up-regulated within 0.5–12 h of heat treatment.

On the other hand, the soluble sugar contents of *R. chinensis* were increased when subjected to heat stress at 2 h–12 h, and decreased during subsequent heat treatment (Additional file 13, Fig. S1c). Consistently, we detected that the expression of genes encoding enzymes involved in starch and sucrose metabolism, fructose and mannose metabolism, as well as galactose metabolism were significantly induced by 2 h–12 h heat treatment, in which genes encoding beta-amylase 1, glucose-6-phosphate isomerase, Glucan endo-1,3-beta-glucosidase 8, Triosephosphate isomerase, Fructose-1, 6-bisphosphatase, galactinol-sucrose galactosyltransferase 5 and Nudix hydrolase 14 were up-regulated within 0.5–6 h of heat treatment. However, the majority of down-regulated genes involved in metabolism were induced at HS\_6 h, and showed a maximal expression level at HS\_12 h (Additional file 9, Table S14).

### 3.10. Hormone regulation-related genes response to heat stress in *R. chinensis*

The comparative transcriptome analysis revealed that many candidate genes involved in hormone biosynthesis, response and signaling, including ABA, auxin, ethylene (ET), gibberellic acid (GA), brassinosteroid (BR), salicylic acid (SA) and jasmonic acid (JA) were regulated by heat stress (Additional file 10, Table S15).

One of the larger DEGs groups was related to ABA. Among these DEGs, most genes involved in ABA response were up-regulated. One gene (contig\_38537) encoding Multiprotein-bridging factor 1c (MBF1C) exhibited the greatest change in expression levels during all heat treatments and was upregulated by 8.72-fold at 2 h<sub>HS</sub>. Five aquaporin PIP2 related genes showed responses to heat treatment on at least one of the treatment times, and four of them were upregulated, especially at the HS\_12 h. Moreover, five genes involved in abscisic acid mediated signaling pathway were also induced by heat treatments. Two of three abscisic acid receptor (PYL4 and PYR1) homologs (contig\_130776 and contig\_30086) were upregulated, while the other one similar to PYL6 (contig\_131618) was down-regulated by 4.06-fold in the 12 h treatment. The expression of three ABA biosynthetic gene, encoding 9-cis-epoxycarotenoid dioxygenase (NCED1, contig\_10795), violaxanthin de-epoxidase (VDE1, contig\_343587) and protein phosphatase 2C (PLL1, contig\_120818) were down-regulated in the 6 h and 12 h heat treatments (Additional file 10, Table S15).

The over-represented GO term 'auxin homeostasis' (GO: 0010252) and 'auxin transport' (GO: 0060918) were found after 12 h of heat treatment. Seven DEGs encoding AUX/IAA proteins were down-

regulated under heat stress, while two genes encoding putative auxin response factor (ARF7 and ARF19) were heat induced, especially ARF7 (contig\_63473), which was induced for more than 4-fold after heat stress treatment of 0.5 h and 2 h. In addition, some DEGs involved in other auxin response and signal, such as homologs of indole-3-acetic acid-induced protein 3 (AGR3), auxin-binding protein 19a (ABP19A), auxin transporter-like protein 3 (LAX3), putative auxin efflux carrier component 8 (PIN8) and CBL-interacting serine/threonine-protein kinase 6 (CIPK6), were downregulated during heat treatments, and most of these genes were initially down-regulated at around 12 h<sub>HS</sub>.

In this study, a large proportion of ethylene biosynthesis and signal transduction genes in the categories ‘ethylene biosynthetic process’ and ‘response to ethylene’ were induced by heat treatments (Additional file 10, Table S15). The homologs of 1-aminocyclopropane-1-carboxylate oxidase 1(ACO) involved in the ethylene biosynthesis process, were significantly upregulated at 2 h–12 h heat treatments. Meanwhile, ethylene signal transduction related genes such as the ET receptor gene ethylene response 1 (ETR1) and ethylene insensitive 3 (EIN3) were up-

regulated under heat treatment for 2–6 h. In addition, several ET signal-related genes, including ethylene response factor ERF8, ERF53, ER-F118,ERF7 and RAP2-10, were upregulated under heat treatment for 2–12 h (Table S9).

All the genes involved in JA-biosynthesis, JA signaling or response were down-regulated, especially by 6 h–12 h heat treatments. Two genes encoding lipoxygenase 2 (LOX2) and allene oxide cyclase 4 (AOC4) were significantly down-regulated more than 4-fold. Moreover, most genes associated with gibberellic acid, salicylic acid, cytokinin and brassinosteroid-related pathways were down-regulated. One gene encoding gibberellic acid-stimulated (GASA2) and one encoding alpha-expansin 6 (EXPA6) that involved in GA-signaling were down-regulated by more than 4-fold (Additional file 10, Table S15).

### 3.1.1. Co-expression network construction and prediction of regulatory circuitry controlling genes in heat stress response

Highly interconnected genes were clustered into one module, and

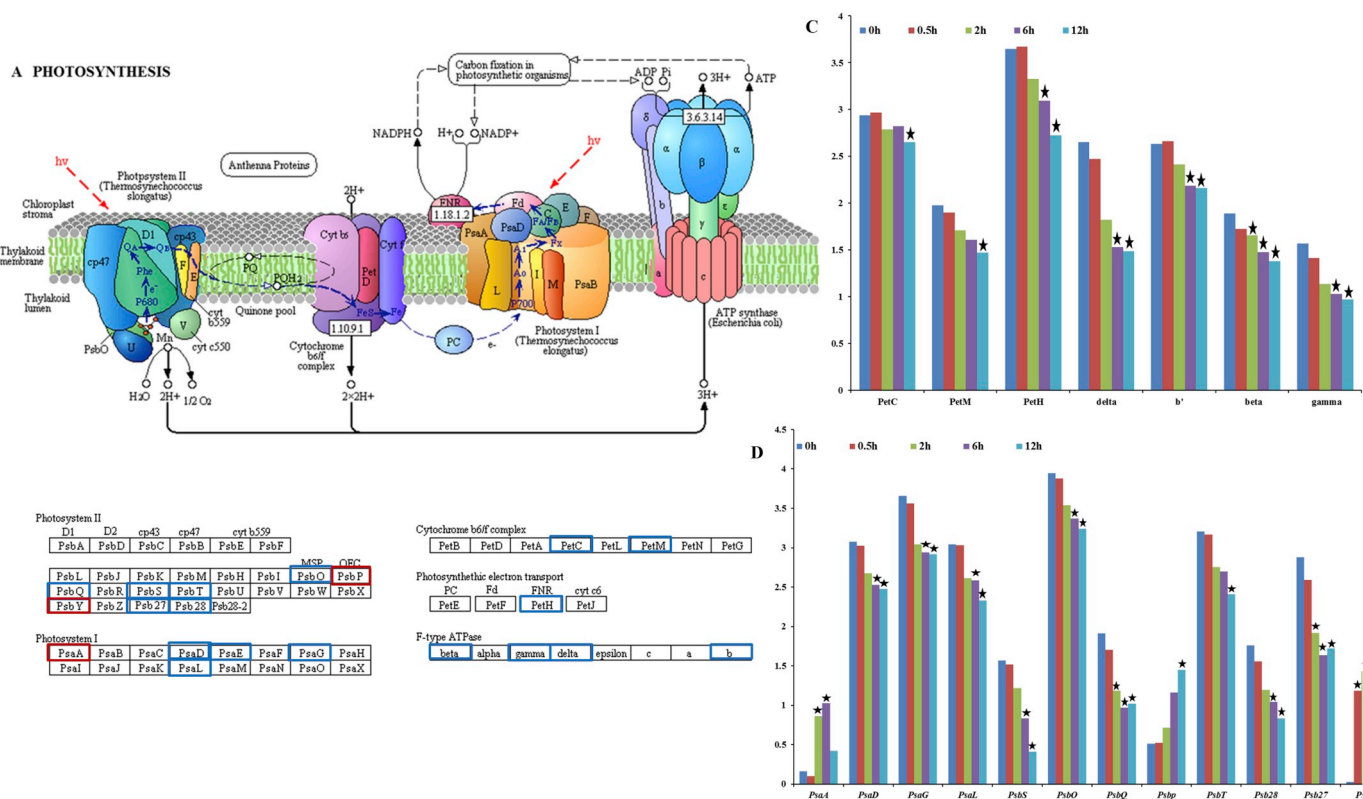


**Fig. 5.** The pathways of photosynthesis (A), and carbon fixation in photosynthetic organism (B) enriched by KEGG analysis. Expression levels of specific genes in the pathways of photosynthesis (C), (D) and carbon fixation in photosynthetic organism (E), (F).

The gene/protein name in a red and blue box represent up-regulation and down-regulation under heat stress, respectively. PsbD, photosystem II oxygen-evolving enhancer protein 1; PsbP, photosystem II oxygen-evolving enhancer protein 2; PsbQ, photosystem II oxygen-evolving enhancer protein 3; PsbS, photosystem II 22 kDa protein; PsbT, photosystem II PsbT protein; PsbY, photosystem II PsbY protein; Psb27, photosystem II Psb27 protein; Psb28, photosystem II 13 kDa protein; PsaA, photosystem I P700 chlorophyll a apoprotein A1; PsaD, photosystem I subunit II; PsaE, photosystem I subunit IV; PsaG, photosystem I subunit V; PsaL, photosystem I subunit XI; PetC, cytochrome b6-f complex iron-sulfur subunit; PetM, cytochrome b6-f complex subunit 7; PetH, ferredoxin-NADP + reductase; Beta, F-type H + -transporting ATPase subunit beta; gamma, F-type H + -transporting ATPase subunit gamma; delta, F-type H + -transporting ATPase subunit delta; b, F-type H + -transporting ATPase subunit b

[EC: 4.1.1.31], phosphoenolpyruvate carboxylase; [EC: 4.1.1.49], phosphoenolpyruvate carboxykinase (ATP); [EC: 1.1.1.37], malate dehydrogenase; [EC: 1.1.1.39], malate dehydrogenase (decarboxylating); [EC: 1.1.1.40], malate dehydrogenase (oxaloacetate-decarboxylating) (NADP+); [EC: 4.1.2.13], fructose-bisphosphate aldolase, class I; [EC:3.1.3.11], fructose-1,6-bisphosphatase II; [EC:3.1.3.37], sedoheptulose-1,7-bisphosphatase; [EC:2.2.1.1], transketolase; [EC:5.3.1.1], triose-phosphate isomerase (TIM); [EC:1.2.1.13] glyceraldehyde-3-phosphate dehydrogenase (NADP +) (phosphorylating); [EC:5.3.1.6], ribose 5-phosphate isomerase A; [EC:5.1.3.1], ribulose-phosphate 3-epimerase; [EC:2.7.1.19], phosphoribulokinase; [EC:5.1.3.1], ribulose-phosphate 3-epimerase; [EC:2.7.2.3], phosphoglycerate kinase; [EC:4.1.1.39], ribulose-bisphosphate carboxylase large chain

Data for the relative expression levels of genes were obtained by DGE data after taking log10 (RPKM + 1). Significant differences compared to the control samples are indicated by asterisks (\*

p < 0.05). (For interpretation of the references to color in this figure legend, the reader is referred to the Web version of this article.)



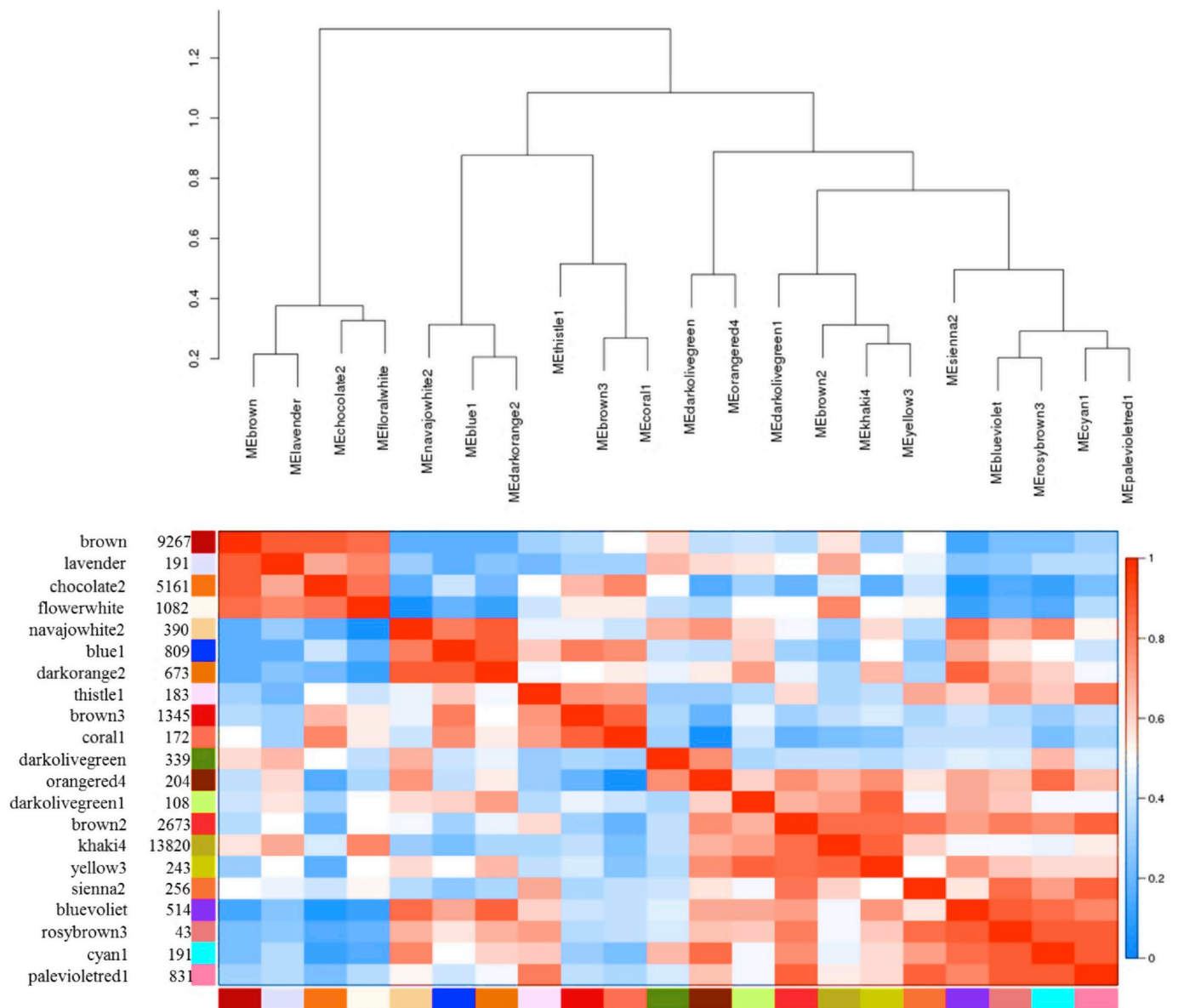


**Fig. 7. Module eigenvector clustering.** The 21 modules were distinguished by different colors assigned by the WGCNA package. The number of genes in each module is indicated on the left. The eigenvectors of each module calculated and clustered using the WGCNA software. The color scale represents the strength of the correlation between the modules (from 0 to 1). (For interpretation of the references to color in this figure legend, the reader is referred to the Web version of this article.)

21 distinct modules were identified. Fig. 7 exhibited the co-expression relationships between modules, which were labeled by different colors. The gene numbers in these modules varied from 43 to 13820, and half of these modules were comprised of more than 500 genes. GO enrichment analysis were conducted for the genes in each module. The significantly enriched GO terms indicated the pivotal biological processes of co-expressed genes, and corroborated our expression analysis of DEGs (Additional file 11, Table S16). For example, genes in the blue1, brown3 and navajowhite2 modules were mainly up-regulated at 0.5–2 h<sub>HS</sub> (Fig. 8A, B, C), and the significantly enriched GO terms of these modules were protein folding, response to stress, response to heat, response to oxidative stress; the brown2 and khaki4 module harbored genes involved in ribosome biogenesis, translation, as well as amino acid biosynthetic and metabolic process, which were mainly up-regulated at 6–12 h<sub>HS</sub> (Fig. 8D and E). While genes in chocolate2 module were mainly down-regulated at 6–12 h<sub>HS</sub> (Fig. 8F), and the significantly enriched functions of this module were carbon utilization, fructose and mannose metabolic process, as well as photosynthesis.

In order to present putative causal regulations between TFs and downstream HS-regulated sub-networks, we tried to link the TFs to their potential binding motifs and co-expressed target genes harboring their binding sites in the transcriptional modules consisting of DEGs unregulated predominately at 0.5–2 h and 6–12 h under heat stress, respectively. The blue1, brown3 and navajowhite2 module exhibited high transcript abundance at 0.5–2 h<sub>HS</sub> included significantly enriched DNA sequence motifs, like ABRE-like, DREBF1-2, DRE-like, Hexamer, ARF, MYB4, LTRE and W-box, mainly associated with TFs, like MYB27, APL, PHL7, BHLH30, BHLH48, BHLH147, WRKY51, bzip12 and MYC1 (Fig. 9A). Target genes with these enriched motifs were associated with enriched GO terms, such as response to heat, protein folding, signal transduction and unfold protein binding (Fig. 9A). TFs like HSFA2, HSFA3, BHLH089, BHLH147, NY-A3, NY-B3 and ERF-RAP2-3 were found in these target genes. The transcriptional module (brown2) of genes showing high expression at 6–12 h<sub>HS</sub> was mainly comprised of significantly enriched DNA motifs, such as ABRE-like, MYB4, DPBF1-2, DRE-like, ARF, MYB3 and MYB, with TFs like PHL7, APL, MYB27,

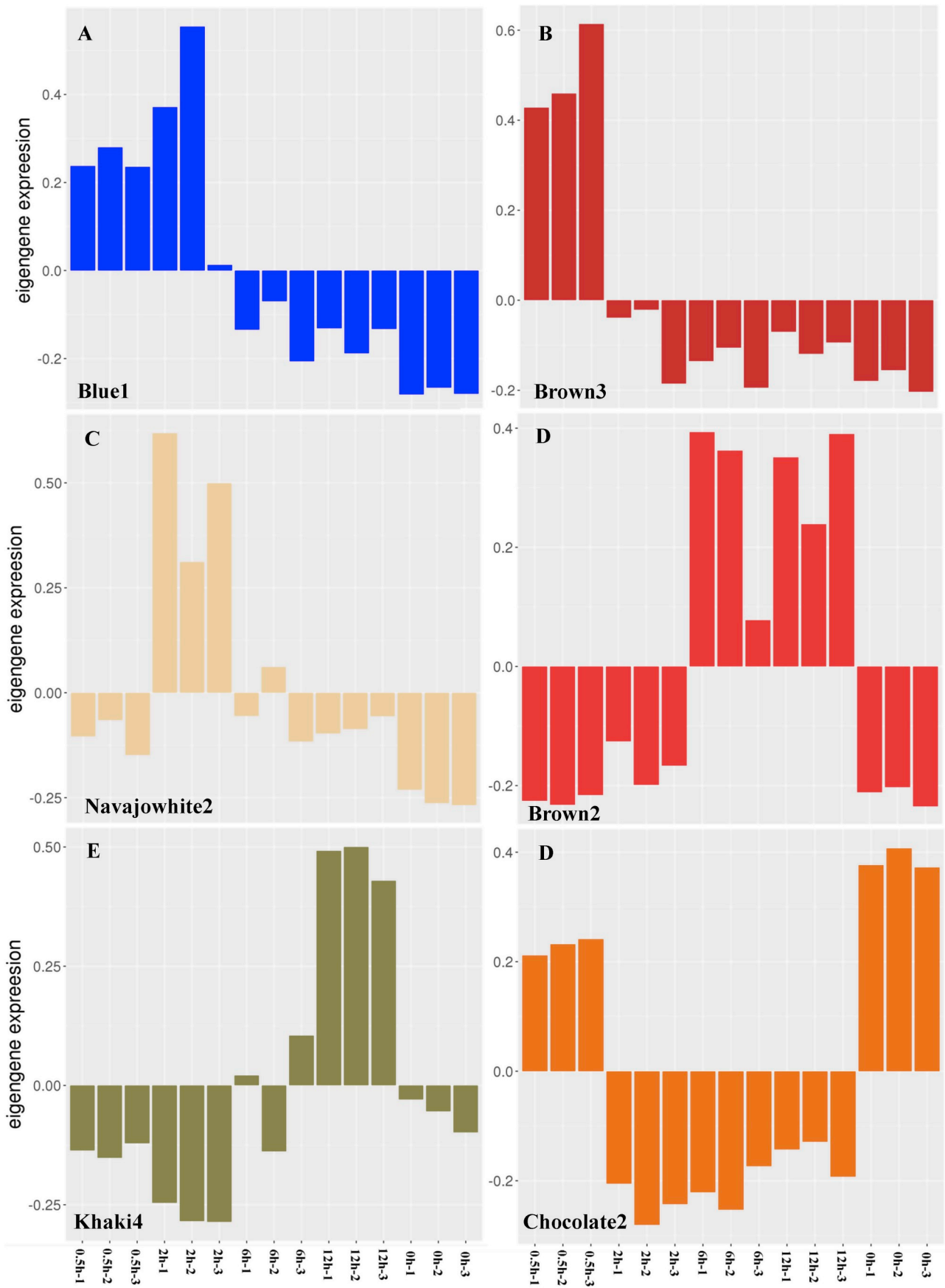
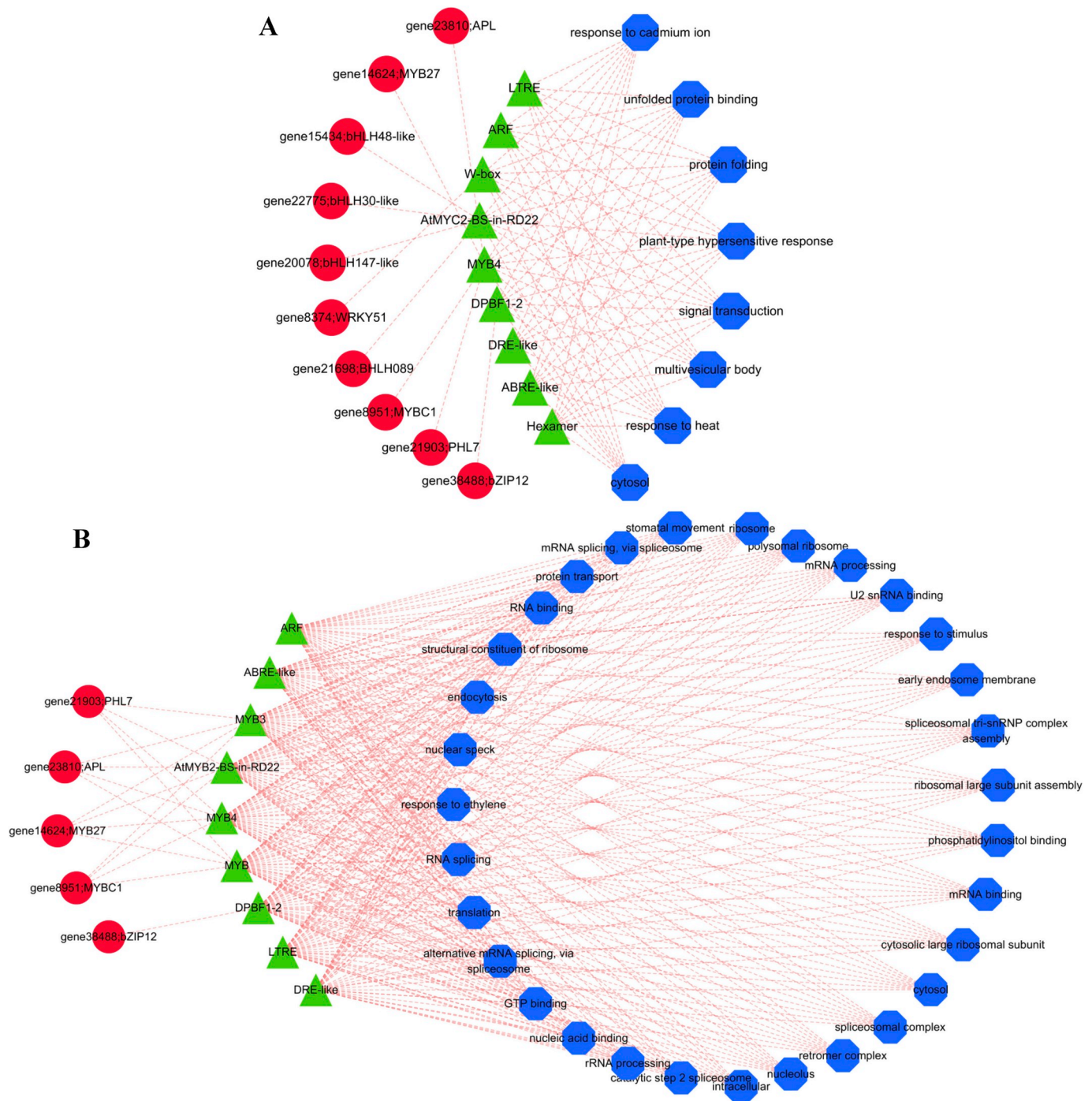


Fig. 8. The expression pattern of the co-expressed genes in the representative module.



**Fig. 9.** The predicted transcriptional regulatory network associated with the modules unregulated predominately at 0.5–2 h (**A**) and 6–12 h (**B**) under heat stress. The significantly enriched cis-regulatory motifs (green triangles) and GO terms (blue hexagons) within the target genes. The TFs are represented by red circles. (For interpretation of the references to color in this figure legend, the reader is referred to the Web version of this article.)

MYBC1 and bzip12 (Fig. 9B). Target genes in this module were involved in stomatal movement, response to ethylene, response to stimulus and translation. TFs like ERF118, DIVARICATA-like, TCP13 and ERF-ABR1-like were found in these target genes.

The blue1 module formed by 809 highly correlated genes highly expressed at 0.5–2 h<sub>HS</sub> (Fig. 8A) strongly attracted our attention. 45 genes in this module encode heat-responsive chaperones, including hsp70-Hsp90 organizing protein, HSPs, Cpn60 and FKBP (ROF). Moreover, TF genes such as *NAC*, *ZAT*, *WRKY*, *MYB* and *HSE*, genes encoding Mitogen-activated protein kinase kinase kinase ANP1 and multiprotein-bridging factor 1c, as well as calcium signaling related

genes including *CDPK*, *CIPK*, *CRT* (calreticulin), were found in this module. The significantly enriched KEGG pathways were ‘Protein processing in endoplasmic reticulum (Ko04141)’ and ‘Cytochrome P450 (Ko00199)’; and the significantly enriched GO terms stress response associated biological processes, cytosolic ribosome, chloroplast and thylakoid related cellular components, as well as protein binding and activity related molecular function (Table 2). The top 50 genes in the blue1 module strongly interconnected with more than 200 edges, were defined as hub genes (Additional file 11, Table S17), including genes encoding 20 kDa chaperonin, chaperonin CPN60-2, chaperone protein ClpB4, HSP70, CBL-interacting protein kinase 2 and peroxidase.

**Table 2**  
GO and KEGG pathway enrichment analysis of blue1 module.

Category	ID	Term	Count	P-value
KEGG_pathway	Ko04141	Protein processing in endoplasmic reticulum	13	6.55391e-09
KEGG_pathway	Ko00199	Cytochrome P450	10	0.0007
GOTERM_BP	GO:0006457	protein folding	37	1.33007e-20
GOTERM_BP	GO:0006950	response to stress	27	1.65990e-17
GOTERM_BP	GO:0009408	response to heat	20	2.69736e-15
GOTERM_CC	GO:0022626	cytosolic ribosome	12	3.01233e-10
GOTERM_CC	GO:0009941	chloroplast envelope	17	4.88514e-08
GOTERM_CC	GO:0009570	thylakoid	6	8.40129e-10
GOTERM_MF	GO:0051082	unfolded protein binding	25	3.76366e-17
GOTERM_MF	GO:0031072	heat shock protein binding	8	6.66059e-07
GOTERM_MF	GO:0001671	ATPase activator activity	4	7.92351e-07

GOTERM\_BP: Gene ontology term biological process; GOTERM\_CC: Gene ontology term cellular component; GOTERM\_MF: Gene ontology term molecular function; KEGG: Kyoto Encyclopedia of Genes and Genomes.

### 3.12. Validation of the differentially expressed genes (DEGs) via RT-qPCR

In order to experimentally validate the expression profile data obtained in this study, the expression patterns of 18 DEGs selected from various functional categories, including transcript factor, heat-responsive protein, and metabolism, were examined via real-time quantitative PCR (qRT-PCR). The expression patterns of all 18 DEGs in the qRT-PCR assays were similar with that in the RNA-Seq data from high-throughput sequencing (Additional file 13, Fig. S2).

## 4. Discussion

### 4.1. Sequence analysis of transcriptome and genome of rose

Recently, the genome sequence of *R. chinensis* ‘Old Blush’ was released (Raymond et al., 2018), which comprises 36,377 inferred protein-coding genes. We mapped our transcriptome data back to the released reference genome, and 27,884 sequences were found to match the whole genome coding sequences, which indicated that our transcriptome data achieved good coverage of the genome. Furthermore, in order to investigate whether the expression profiles analysis of these key genes in our paper were similar to the analysis performed with rose reference genome, we calculated the correlation of the RPKM of the key genes analyzed in our paper between the de novo assembly data and reference genome data. The correlation between these two data was high and no significant difference were found (Additional file 13, Fig. S3).

### 4.2. Different signaling pathways mediate early heat stress response

Upon short-term exposure to environmental stress, plants could trigger multiple signal transduction pathways, which can activate the expression of stress-responsive genes and regulate numerous downstream metabolic networks responsible for physiological adaptation (Fu et al., 2016).  $Ca^{2+}$  mediated signaling has been proved to universally participate in multiple stress responses in plants (Reddy et al., 2011). Previous studies have shown that heat stress stimuli can rapidly and transiently elevate the cytosolic  $Ca^{2+}$  concentration in many plants, which are sensed by several  $Ca^{2+}$  sensors or  $Ca^{2+}$  binding proteins (CBP), such as calmodulin (CaM), CaM-related proteins,  $Ca^{2+}$ -dependent protein kinases (CDPK) and calcineurin B-like protein (CBL) (Qin et al., 2008; Wan et al., 2015; Yan et al., 2016). CDPKs/CPKs are the essential primary  $Ca^{2+}$  sensors in plants and have been shown to play a vital role in plant abiotic stress responses (Zou et al. 2010, 2015; Valmonte et al., 2014; Dubrovina et al., 2017). In *Arabidopsis*, CPK13 function as positive regulators of the expression of HSP genes (*HSP70*, *HSP101*, *HSP17.4* and *HSP15.7*) and involve in HS tolerance (Nagamangala et al., 2010). In this study, four genes encoding putative  $Ca^{2+}$ -dependent

protein kinase showed a high expression level at the 0.5–6 h heat treatment time points, and two of them are putative CPK13 gene. Similarly, the expression of *HSP70*, *HSP101* and *HSP15.7* genes also were induced by heat stress at all four time points. These results indicated that  $Ca^{2+}$  mediated CDPK pathway had been activated as short as 0.5 h of heat stress treatment in *R. chinensis*. Moreover, CBL proteins were found to form a complex network with their target kinases named CBL-interacting protein kinase (CIPK), and the CBL–CIPK pathway has been shown to be involved in various abiotic stresses responses, such as cold, heat, drought and salinity (Zhao et al., 2009; Luan, 2009; Yu et al., 2014; Thoday-Kennedy et al., 2015). In this study, two DEGs encoding CIPK2 and CIPK9 were differentially up-regulated at 0.5 h–2 h HS, which indicated that CBL–CIPK pathway may contribute to the regulation of early heat response in *R. chinensis*.

Additionally, another prominent signal transduction pathway detected in this study was the ‘MAPK signaling pathway’. MAPK cascades are ancient and conserved signaling cassettes that play a pivotal role in the activation of defense responses in plants (Gohar et al., 2010). Kovtun et al. (2000) found that constitutively active Arabidopsis mitogen-activated protein kinase kinase ANP1 (DANP1), which can mimic the  $H_2O_2$  signal and induce the GST6 promoter, enhanced tolerance to multiple environmental stress conditions including heat stress. In this study, one gene encoding ANP1 and one gene encoding GST6 were all significantly upregulated during 0.5–2 h heat treatments. This suggested that protein phosphorylation involving mitogen activated protein kinases might participate in the transduction of oxidative signals and in the early response to heat stress in *R. chinensis*.

Previous studies have indicated that modification of the expression of heat shock genes related to the biosynthesis of osmoprotectants would improve heat tolerance of plants; the production of the soluble sugars induced by heat stress could regulate the levels of osmoprotectants in plants (Qin et al., 2008; Mangelsen et al., 2011). In *R. chinensis*, the soluble sugars content was increased from 0.5 h to 12 h heat treatment. Parallel comparative transcriptome analysis revealed that the expression level of genes related to the biosynthesis of soluble sugars was modified by heat stress after 6 and 12 h of exposure. For example, genes encoding galactinol-sucrose galactosyltransferase 5 and UDP-glucose 4-epimerase, involved in the production of raffinose and galactinol (Nishizawa et al., 2008; Mangelsen et al., 2011), were up-regulated by heat stress at 6–12 h. Galactinol and raffinose have been proved to function as osmoprotectants in stress tolerance of plants (Taji et al., 2010; Mangelsen et al., 2011). Whilst the expression level of genes encoding beta-amylase 1 and nudix hydrolase 14 involved in the starch degradation were elevated at 2 h–12 h (Radchuket al. 2009; Muñoz et al., 2006), and the repression of several genes involved in the biosynthesis of starch were started from 6 h to 12 h, which indicated that the negative impact of heat stress on the starch biosynthesis was induced as short as 6 h of heat stress treatment. In addition, heat stress induced the expression of genes mediating in sucrose transport pathways. Genes encoding sugar transport proteins and hexose transporter, which are regulated by the hexokinase independent sugar transduction pathway and participated in phloem loading of sugars (Gupta and Kaur, 2005; Cordoba et al., 2015), were strongly induced at 2–12 h. While gene encoding fructokinase, related to sugar sensing bypass hexokinase phosphorylation in plants (Gupta and Kaur, 2005), was upregulated at 12 h. Thus, our results suggested that sugar signaling may be triggered as short as 2 h of heat stress treatment in order to repress and/or redirect the sugar utilization.

### 4.3. Heat shock proteins function as predominant regulators mediating in the heat shock response

Transcriptome profile analysis in many plants under heat stress indicated that a significant fraction of most strongly upregulated DEGs encode molecular chaperones (Liu et al., 2012; Wan et al., 2015; Yan et al., 2016). Consistently, numerous heat-induced chaperones were found to be upregulated in this study, including heat shock proteins (HSPs), peptidyl prolyl cis/trans isomerase and BAG protein family, and HSPs were the most predominant chaperones.

As the universal molecular chaperone, HSPs can help other proteins maintain their native conformation and improve their stability under stresses. Previous studies indicated that HSPs-mediated protein folding represented one of predominant processes in plants that resulted from a short-term heat stress treatment (Mangelsen et al., 2011; Jung et al., 2012; Wan et al., 2015). In this study, most of the HSPs were consistently up-regulated at all four time points, and exhibited the highest expression level at 0.5–2 h, which pointed that HSPs-mediated protein folding participated in the initial and major processes in response to heat stress in *R. chinensis*.

To date, five structurally distinct classes of HSPs have been characterized in plants, based on their molecular weight. These classes are Hsp100, Hsp90, Hsp70, Hsp60 and small HSPs (sHSPs) (Kotak et al., 2007). Previous studies showed that chloroplast and mitochondrial sHSPs can protect plants against heat stress and enhance thermos-tolerance in plants (Heckathorn et al., 1998; Sanmiya, 2004). While Jiang et al. (2009) found that RchHSP17.8, a cytosolic class I small HSP characterized from *R. chinensis* ‘Sohloss Mannieim’, was able to confer heat resistance to *A. thaliana*. In this study, 26 members of the sHSP family, including mitochondrial, chloroplast, and cytosolic sHSPs, were highly induced by heat stress at all four time points. The expression level of most of these sHSPs were higher than those of Hsp70, Hsp90 and Hsp100, and *Hsp17.8* were the highest expression members of all HSPs, which suggested that sHSPs are the most important gene candidates to improve stress responses with positively affecting different cellular compartments of leaves in *R. chinensis*. On the other hand, recent findings specified that sHSPs act as ATP independent chaperones to prevent the aggregation of misfolded proteins by cooperating with HSP70 protein (Lee and Vierling, 2000; Frank et al., 2009). The *HSP70* genes were proved to be the responsible for HS and play a protective role in thermo-tolerance in many plant species (Su and Li, 2008; Mulaudzi-Masuku et al., 2015; Guo et al., 2016). 48 genes encoding HSP70 protein also has been found to be significantly up-regulated under heat stress in our study, which also provided a series of interesting candidate genes to reduce negative effects on the growth of rose. Additionally, cytosolic ClpB1 (At1g74310), better known in Arabidopsis as AtHsp101, was also one of the best-studied HSP proteins in plants, which was found to play a crucial role in heat stress tolerance in plants (Lee et al. 2005, 2007). The putative gene encoding Hsp101 in this study was induced by more than 8-fold when given a heat treatment for 0.5–2 h. Combined with co-expression results that most hub genes were annotated as HSPs, the accumulated data in our study thus indicated that HSPs-based protection mechanism of *R. chinensis* was quickly induced by short-term heat stress and played an important role in early modification of HSR.

#### 4.4. Candidate transcription factor for the modification of heat stress response in *R. chinensis*

Previous studies in Arabidopsis and tomato have highlighted the vital regulatory roles of HSF family in the transcriptional regulatory network of the HSR (Koskull-döring et al., 2007a,b; Ohama et al., 2017). Among these HSFs, the function of HSF2 in tomato and Arabidopsis were well documented. Arabidopsis AtHsfA2 and tomato LeHsfA2 (*HSF30*; Baniwal et al., 2004) are all HS-inducible and expressed at a high level after heat stress treatment, and served as the dominant HSF gene for thermos-tolerance in both tomato and Arabidopsis (Koskull-döring et al., 2007a,b). Consistently, we found that the expression of rose *HsfA2* (*HSF30*) (contig\_245724) was strongly induced at each of the four heat treatment time points, which provide evidence that HsfA2 was also the dominant transcription factor in the regulation of rose heat stress responses. Additionally, Meiri and Breiman (2009) found that in Arabidopsis, HsfA2 could interact with HSP90 and help the ROF1–HSP90 complex to translocate into the nuclear under heat stress, and the localization of the ROF1–HSP90 complex would modulate thermos-tolerance of Arabidopsis; meanwhile HsfA2 and ROF1 could synergistically affect the accumulation of sHSPs. Interestingly, *ROF1* gene, as well as several *HSP90* and *sHSPs* genes were also highly induced by more than 8-fold with heat treatment for more than 0.5 h in this study, which

suggested that the regulation mode of HsfA2, ROF1 and HSP90 may exist in *R. chinensis*, and can regulate the expression of some genes under heat stress. In Tomato and Arabidopsis, A4Hsfs act as the potent activator of heat stress gene expression in HsfA1-independent pathways, and HsfA4a serves as a sensor of reactive oxygen species (ROS) produced during heat stress, whereas HsfA5 is proved to be a specific repressor of HsfA4 upon attenuation of the ROS signal (Baniwal et al., 2007). In our study, the expression level of rose *HsfA4a* was significantly increased only by 2 h HS treatment, while rose *HsfA5a* showed elevated expression from HS\_2 h to HS\_12 h, which suggested that heat stress may produce oxidative stress in the early stage, and rose *HsfA4a* and *HsfA5a* may contribute to the regulation of ROS signaling pathway under heat stress. Comparing with class A Hsfs, the function and regulation mode of class B Hsfs were the least understood (Koskull-döring et al., 2007a,b). AtHsfB1 and AtHsfB2b act as repressors of class A Hsfs and HSPs under non-heat-stress conditions, but positively regulate the expression of HS-inducible HSPs (*HSP101*, *sHSPs*, *HSP70* and *HSP90*) and the acquired thermos-tolerance under heat stress (Ikeda et al., 2011). In this study, we found that the expression of *HsfB2b* (contig\_60744) and *HsfB1* (contig\_243625) were all increased during heat stress treatments. Correspondingly, most of rose *HSP101*, *sHSPs*, *HSP70* and *HSP90* exhibited a higher expression level at HS\_2 h, which indicating that rose *HsfB2b* and *HsfB1* would also positively regulate the expression of HSPs under heat stress in *R. chinensis*. Summarized, our results suggested that Hsfs may be the crucial master regulators in the early HSR in *R. chinensis*, and the transcriptional regulatory network of rose Hsf family in the response to heat stress remains a subject for future research. In addition to HSFs, *DREB2C* and *AtNAC019* was observed to be required for thermo-tolerance in Arabidopsis. The *DREB2C* overexpression transgenic Arabidopsis plants are found to be more heat tolerance than the wild type (Lim et al., 2007), and *DREB2C* was proved to function as a transcriptional activator of AtHsfA3 during the heat stress response (Chen et al., 2010); while AtNAC019 can positively affect the expression of several HS-inducible genes (e.g. *HsfA1b* and *HsfB1*) and is critical for thermos-tolerance (Guan et al., 2014). In this study, the high expression level of *DREB2C* and HsfA3 was detected at all four time point, and the expression levels of rose *NAC019* and *HsfB1* were significantly increased after 2 h of heat stress, which points to the critical regulatory role of *DREB2C* and *NAC019* in the heat shock response in *R. chinensis*. Except *NAC019*, 18 DEGs similar to *NAC/NAM* positively induced by heat stress in this study, and 16 ones were rapidly up-regulated after 2 h of heat stress, which indicated that *NAC/NAM* family also acted as regulatory components in early HSR in *R. chinensis*. In Arabidopsis, AtNAC072 are shown to mediate in the ABA-responsive gene regulation (Li et al., 2016). Moreover, *NAC072* and *NAC029* were shown to be HS-inducible and participate in ABA signaling in *R. hainanense* (Zhao et al., 2018). The up-regulation of rose *NAC29* and *NAC72* indicated that the ABA signaling may participate in the HSR in *R. chinensis*.

Moreover, we performed co-expression network and transcription regulatory modules analysis and tried to identify TFs associated with downstream HS-regulated subnetworks. Members of HSF and NAC families were identified in the modules involved in ‘response to heat’, ‘protein folding’, ‘signal transduction’ and ‘unfold protein binding’, which indicated that they act as regulatory components to coordinate the activity of co-expressed genes in these modules. In addition to them, the potential binding motifs of some members of MYB, BHLH, WRKY and bZIP family, such as MYB27, APL, PHL7, BHLH30, BHLH48, BHLH147, WRKY51 and bzip12 were identified to be enriched in these modules, which highlighted that these TFs may be able to regulate the downstream target genes participating in signal transduction and response to heat. Certainly, further functional studies on these TFs are required to elucidate the gene regulatory network of heat stress response in *R. chinensis*.

#### 4.5. ROS-scavenging was one of the predominant processes in heat stress response

Heat stress will lead to the over accumulation of reactive oxygen species (ROS), which can cause oxidative damage to plant cell

membranes, DNA and proteins. In order to maintain normal cellular functions, plants will try to reduce ROS levels and oxidative stress by enhancing the antioxidant enzyme system (Miller et al., 2008; Gill et al., 2010). To date, many ROS-scavenging enzymes have been found to be elevated by heat stress in plant, and help plants to acquire thermo-tolerance, including superoxide dismutase (SOD), catalase (CAT), guaiacol peroxidase (GPX), ascorbate peroxidase (APX), and glutathione (GSH) (Vacca et al., 2004; Qin et al., 2008; Song et al., 2014; Ara et al., 2015). In this study, we identified some DEGs encoding putative respiratory burst oxidase, ferric reduction oxidase, polyphenol oxidase, glycolate oxidase and amine oxidases, which are involved in ROS production (Mittler et al. 2004). Among these ROS production related genes, only one putative amine oxidase gene was upregulated by 0.5–2 h heat stress, but the other genes related to ROS production were repressed by treatments of 6–12 h, indicating that amine oxidase may be the main producer of signal transduction-associated ROS in cells of *R. chinensis*. In contrast, most of the DEGs encoding antioxidants, including ascorbate peroxidase (APX), glutathione S-transferase, ferritin, thioredoxin and NADPH-cytochrome P450 reductase, showed high expression levels after 0.5 h of heat stress, especially at the 2 h heat treatment, suggesting that these antioxidants primarily served as the scavengers of HS-induced ROS in *R. chinensis*. While gene encoding superoxide dismutase was up-regulated after 12 h of heat stress, and the SOD activity was significantly increased after 6 h of heat stress but decreased from 16 h to 24 h, which indicated the slow response and poor stability of SOD in *R. chinensis* during heat stress.

#### 4.6. Photosynthesis was negatively regulated by short-term heat stress

Photosynthesis, an essential metabolic process for plant growth and development, is very sensitive to heat stress (Allakhverdiev et al., 2008), and the photosystem was identified as one of the most stress-sensitive sites in the photosynthetic machinery (Schrader et al., 2004; Song et al., 2014). In this study, the significant reduction of *Fv/Fm*, *Fv'/Fm'* and ETR demonstrated that the injury of high temperature on photosynthetic electron transport system in *R. chinensis* happened after 24 h of exposure. Meanwhile, comparative transcriptome analysis revealed that more genes involved in photosynthetic electron transport system were down-regulated than up-regulated, and many key genes related to PS I, PS II and redox chain, such as oxygen-evolving enhancer protein, chlorophyll *a-b* binding protein, PS I reaction center subunit and cytochrome *b6-f* complex subunit, were down-regulated after 6 h of heat exposure, which suggested that the thermal inactivation of photosynthetic electron transport system may be the result of very early impairment of multi-subunit protein complexes. Interestingly, although most genes related to PS I, PS II and redox chain were down-regulated by heat stress, we also found several genes encoding crucial factors involved in protection of photosystems were up-regulated under heat stress treatment. For example, the gene encoding PsbP, which is necessary for the maintenance and assembly of PSII in higher plants (Ifuku et al. 2005), was up-regulated at 6 h of heat treatment; and the gene encoding PsbY, which was suggested to prevent PSII from photodamage (Sydow et al. 2016; Plöschinger et al. 2016), was significantly up-regulated by more than 6-fold from 2 h to 12 h heat treatment in this study. In addition, rose *PGR5* gene was up-regulated significantly after 6 h of heat stress treatment in this study. *PGR5* (PROTON GRADIENT REGULATION) is essential for photoprotection, as it can help to maintain the correct production ratio of ATP/NADPH and regulate the cyclic electron flow of PSI (Munekage et al., 2002; Long et al., 2008). PSI cyclic electron flow is proved to be crucial for protecting both PSII and PSI from photodamage caused by environmental stress (Ivanov et al., 2017). Paredes and Quiles (2013) found that when exposed to heat stress condition, *PGR5*-dependent PSI cyclic electron flow was also up-regulated in a heat tolerance *Rosa* species, *R. meilandina*. Thus, based on our data, *PGR5*, *PsbY* and *PsbP* may be gene candidates and can improve HSR without negatively affecting photosynthetic electron transport system in *R. chinensis*.

Heat stress adversely affects photosynthesis in plants not only by

disruption of photosynthetic electron transport system, but also by modulation of photosynthetic carbon fixation (Allakhverdiev et al., 2008). In this study, the general repression of genes related to Calvin cycle were occurred after 6 h of heat stress treatment, which suggested that the negative effects on photosynthetic carbon fixation cycle might be initiated after as short as 6 h of heat stress. Previous studies observed that the activity of RuBisCO subunits would be significantly inhibited by high temperature (over 40 °C) after as short as 2 h of exposure (Ahsan et al., 2010; Song et al., 2014), and the inactivity of the Rubisco at high temperature is due to Rubisco activase (RCA), which is extremely sensitive to heat stress and act as a major limiting factor in plant photosynthesis under heat stress (Kurek et al., 2007). Consistently, our results showed that genes encoding RuBisCO small chain and RCA1 were downregulated after 6 h of heat stress. By contrast, gene encoding phosphoribulokinase (PRK), which is involved in the re-generation of RuBisCO, was highly induced at 0.5 HS; while genes encoding CPN-60, which served as prototypical chaperon binding RuBisCO small and large subunits in plants, were significantly up-regulated at 0.5 HS and 2 h HS. CPN-60 is involved in PSII repair and can protect rubisco activase from thermal denaturation (Dobrá et al., 2015). Thus, the significant up-regulation of *CPN-60* and *PRK* under heat shock indicated that the fast stimulation of defense mechanisms may be activated after as short as only a few hours of heat stress treatment in *R. chinensis*. In addition, we also found that gene encoding Calvin cycle protein (CP12), which have a role in determining the level of phosphoribulokinase and photosynthetic capacity (Elena et al., 2017), was up-regulated at all four different time points; and genes encoding fructose-bisphosphate aldolase (SCA1), was stress-inducible and can improve the survival ability of plants under stress (Zeng et al., 2015). As CP12 and SCA1 gene coding proteins involved in protection of photosynthetic carbon fixation, they also may act as the gene candidates to improve heat stress responses without adversely affecting photosynthesis in *R. chinensis*.

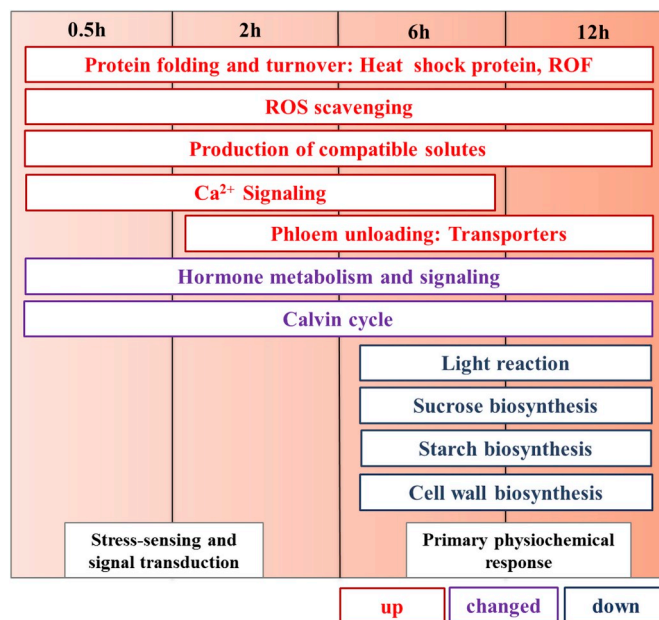


**Fig. 10.** Summary of heat responsive processes in *R. chinensis*. Functional groups of induced and repressed genes at 0.5, 2, 6 and 12 h of heat exposure are depicted as blue and red boxes, respectively. Functional groups containing both induced and repressed genes are depicted as purple boxes. The length of the boxes is indicative for the duration of induced or repressed expression levels over just one or several investigated time points. Two different phases of heat response, named sensing and signal transduction, primary heat response, were defined at the bottom. (For interpretation of the references to color in this figure legend, the reader is referred to the Web version of this article.)

#### 4.7. Abscisic acids, ethylene and MBF1c may involve in the regulation of heat stress response

Although abscisic acids (ABA) have been known to play an important role in enhancing abiotic stresses tolerance in plants (Vishwakarma et al. 2016), the role of ABA in HSR were not consistent in different plants species. Recent reports in *A. thaliana* (Dobrá et al., 2015) revealed that when the whole plants were subjected to severe heat shock for 2 h, a decrease of ABA content correlated with a down-regulation of ABA biosynthetic genes (*NCED*) was observed in leaves. Consistently, several ABA biosynthesis genes (*NCED*, *VDE*) were significantly down-regulated in leaves of *R. chinensis* after 6 h of heat stress. In addition, Zandalinas et al. (2016) indicated that tolerance of citrus plants to heat stress is associated with ABA reduction in photosynthetic organs, which is a necessary response to the stimulation of transpiration. In this study, the transpiration rate was increased from 2 h to 6 h heat treatment (data not shown). Thus, our results supported the assumption that the reduction of ABA in leaves is a necessary response to enhance transpiration which served as a direct response to the heat stress.

In addition to ABA, recent studies have also shown that ethylene also serves as a stress-related hormone in plants: ethylene insensitive and signaling Arabidopsis mutants exhibited stronger defects in thermo-tolerance (Larkindale and Knight, 2002; Larkindale et al., 2005). In this study, we identified several candidate genes involved in ethylene biosynthesis/signaling in *R. chinensis*, such as genes encoding ACO, EIN3, ethylene receptor ETR1, and several ERF proteins, which suggested that the ethylene pathway is involved in the early regulation of HSR in *R. chinensis*. Ethylene receptor ETR1 and EIN3 served as the downstream components of the ethylene receptor play a crucial role in ethylene signaling pathway in plants (Yoo et al., 2008). Arabidopsis ethylene

signaling mutants, *ein2* and *etr1*, were reported to be more defective in basal thermo-tolerance (Larkindale et al., 2005). Thus heat stress-induced ethylene biosynthesis/signaling in *R. chinensis* may be an interesting research direction for heat resistant improvement and based on our results, *ETR1* and *EIN3* may act as gene candidates to improve early HSR without negative effects in *R. chinensis*.

Additionally, some research suggested that MBF1c served as a crucial regulator of thermo-tolerance in *A. thaliana* and functioned upstream to ethylene during heat stress; the constitutive expression of *MBF1c* has been shown to enhance thermo-tolerance of transgenic plants by elevating a number of transcripts involved in ethylene signal pathway, including ethylene response-binding factors (ERF) (Suzuki et al., 2005). Moreover, Suzuki et al. (2011) found that MBF1c can elevate the expression of two *Hsfs* (B2a and B2b). In accord with these reports, we found that one DEG annotated as MBF1c (contig\_38537) exhibited elevated expression at four time points of heat stress; while two *Hsfs* (B2a and B2b) and several *ERFs* showed a higher expression level after 2 h of heat stress, which indicated that MBF1c may serve as one crucial heat stress-response regulator of *R. chinensis*.

## 5. Conclusion

To our knowledge, this is the first study that provides a comprehensive and detailed analysis of the transcriptomic and physiochemical responses of *R. chinensis* to heat stress. Combined with physiochemical and transcriptomic data, the predominant processes in *R. chinensis* that resulted from the short-term heat exposure were summarized in Fig. 10. Chaperone-mediated protein folding, ROS scavenging and production of compatible solutes were the major processes of HSR, which were rapidly and consistently up-regulated at all four time points. In parallel, the expression of genes involved in  $Ca^{2+}$  signaling and sugar

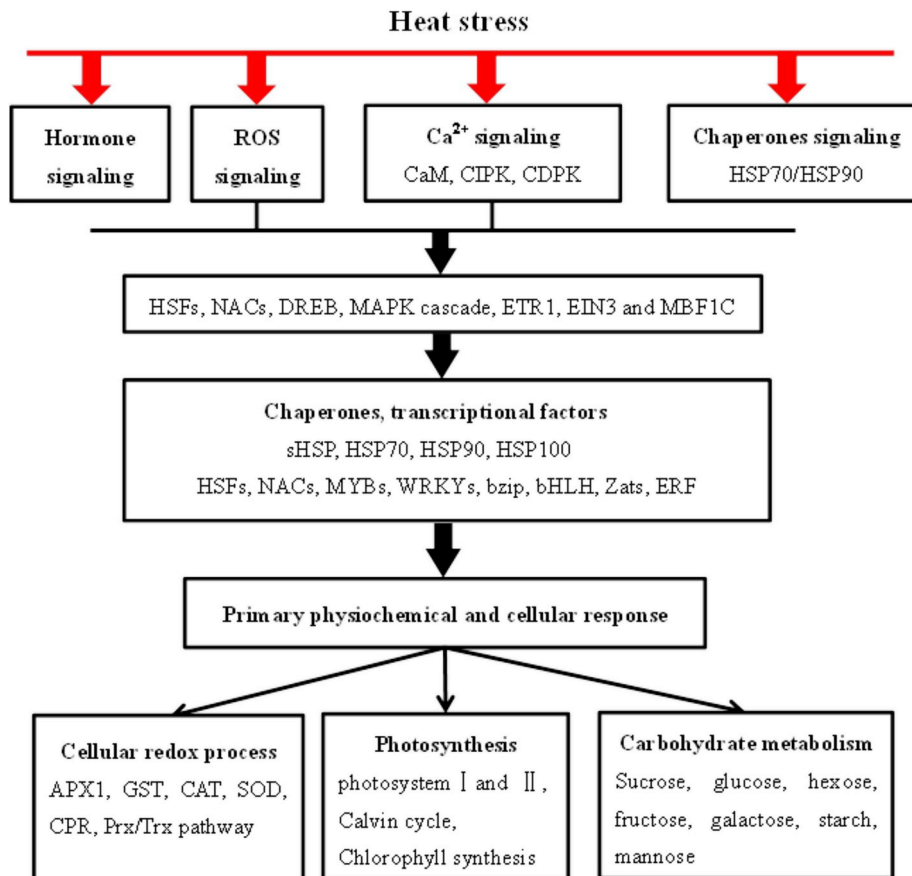


Fig. 11. Hypothetical model summarizing the events occurring in leaves of *R. chinensis* upon heat stress.

transporters, as well as hormone metabolism and signaling were quickly altered after 0.5–2 h of heat treatment, which indicated the rapid sensing and signal transduction of early HSR in *R. chinensis*. On the other hand, the expression of most genes related to light reaction, sucrose biosynthesis, starch biosynthesis and cell wall biosynthesis were reduced after as short as 6 h of heat stress, which indicated the ongoing negative effects on the physiology of *R. chinensis*. In summary, the early HSR in *R. chinensis* could be represented by two distinct phases: ‘stress-sensing and signal transduction’ and ‘primary physiochemical response’. The heat-responsive model of *R. chinensis* could be summarized in Fig. 11. The heat stress may transduce via calcium, chaperones, ROS and hormone signaling, which would quickly activate multiple regulons, such as certain HSFs, NACs, MYBs, ROF1, MBF1c, CDPK, as well as MAPKs. The action of these heat responsive regulons will trigger the expression of a cascade of genes encoding chaperones, transcription factors and multiple enzymes, which further modulate cellular metabolic homeostasis. These candidate genes and factors involved in heat regulation of the Ca<sup>2+</sup> and ROS signaling pathways, ABA and ethylene related pathways, photosynthesis, as well as carbohydrate metabolism could facilitate future studies on the molecular mechanisms of heat stress tolerance in rose.

### Conflicts of interest

The authors declare that they have no conflict of interest.

### Author contributions statement

ZeQing Li: Conducted the majority of the experimental work with technical help and revised the manuscript; Wen Xing: Conducted and design the experiments, analyzed the experimental data, and wrote the manuscript; Ping Luo: Contributed to revising manuscript. JingFang Zhang, Minhuan Zhang and LingXiao Jin: Conducted the majority of the physiology experimental work.

### Acknowledgments

This research was supported financially by the National Natural Science Foundation of China (31501794), the Natural Science Foundation of Hunan province (2018JJ3879), China Postdoctoral Science Foundation (2019M652816), the State Forestry Administration of the “13th Five-Year” key discipline No.[2015]44, as well as the key discipline of Hunan Province in 12th Five-Year ([2011]76). The authors thank Wuhan Igenebook Biotechnology Co., Ltd (Wuhan, China) for technical support.

### Appendix A. Supplementary data

Supplementary data to this article can be found online at <https://doi.org/10.1016/j.plaphy.2019.07.002>.

### References

Ahsan, N., Donnart, T., Nouri, M.Z., Komatsu, S., 2010. Tissue-specific defense and thermo-adaptive mechanisms of soybean seedlings under heat stress revealed by proteomic approach. *J. Proteome Res.* 9, 4189–4204. <https://doi.org/10.1021/pr100504j>.

Allakhverdiev, S.I., Kreslavski, V.D., Klimov, V.V., Los, D.A., Carpentier, R., Mohanty, P., 2008. Heat stress: an overview of molecular responses in photosynthesis. *Photosynth. Res.* 98, 541. <https://doi.org/10.1007/s11120-008-9331-0>.

Ara, N., Nakkanong, K., Yang, J.H., Hu, Z.Y., Zhang, M.F., 2015. Dissecting the heat stress-induced alterations in the leaf ultrastructure and some antioxidant network components in interspecific (*Cucurbita maxima* × *Cucurbita moschata*) inbred line of squash ‘Maxchata’ as to its parents possessing variable heat tolerance. *Plant Growth Regul.* 76, 289–301. <https://doi.org/10.1007/s10725-015-0024-3>.

Baniwal, S.K., Bharti, K., Chan, K.Y., Fauth, M., Ganguli, A., Kotak, S., et al., 2004. Heat stress response in plants: a complex game with chaperones and more than twentyheat stress transcription factors. *J. Biosci.* 29, 471–487. <https://doi.org/10.1007/BF02712120>.

Baniwal, S.K., Chan, K.Y., Scharf, K.D., Nover, L., 2007. Role of heat stress transcription factor HsfA5as specific repressor of HsfA4. *J. Biol. Chem.* 282, 3605–3613.

Baron, K.N., Schroeder, D.F., Stasolla, C., 2012. Transcriptional response of abscisic acid (ABA) metabolism and transport to cold and heat stress applied at the reproductive stage of development in *Arabidopsis thaliana*. *Plant Sci.* 188–189, 48–59. <https://doi.org/10.1016/j.plantsci.2012.03.001>.

Chen, H., Hwang, J.E., Lim, C.J., Kim, D.Y., Lee, S.Y., Lim, C.O., 2010. Arabidopsis dreb2c functions as a transcriptional activator of hsf3 during the heat stress response. *Biochem. Biophys. Res. Commun.* 401, 0–244. <https://doi.org/10.1016/j.bbrc.2010.09.038>.

Chen, L., Han, Y., Jiang, H., Korpelainen, H., Li, C., 2011. Nitrogen nutrient status induces sexual differences in responses to cadmium in *populus yunnanensis*. *J. Exp. Bot.* 62, 5037–5050. <https://doi.org/10.1093/jxb/err203>.

Cordoba, E., Aceveszamudio, D.L., Hernándezbernal, A.F., Ramosvega, M., León, P., 2015. Sugar regulation of sugar transporter protein 1 (stp1) expression in *arabidopsis thaliana*. *J. Exp. Bot.* 66, 147–159. <https://doi.org/10.1093/jxb/eru394>.

Dobrá, J., Černý, M., Štorchová, H., Dobrev, P., Skalák, J., Jedelský, P.L., et al., 2015. The impact of heat stress targeting on the hormonal and transcriptomic response in *Arabidopsis*. *Plant Sci.* 231, 52–61. <https://doi.org/10.1016/j.plantsci.2014.11.005>.

Duan, B.L., Lu, Y.W., Yin, C.Y., Junttila, O., Li, C.Y., 2005. Physiological responses to drought and shade in two contrasting *Picea asperata* populations. *Physiol. Plantarum* 124, 476–484. <https://doi.org/10.1111/j.1399-3054.2005.00535.x>.

Dubrovina, A.S., Kiselev, K.V., Khristenko, V.S., Aleynova, O.A., 2017. The calcium-dependent protein kinase gene VaCPK29 is involved in grapevine responses to heat and osmotic stresses. *Plant Growth Regul.* 82, 79–89. <https://doi.org/10.1007/s10725-016-0240-5>.

Elena, L.P., Omar, A.A., Lawson, T., Anne, R.C., 2017. Arabidopsis CP12 mutants have reduced levels of phosphoribulokinase and impaired function of the Calvin-Benson cycle. *J. Exp. Bot.* 68, 2285–2298. <https://doi.org/10.1093/jxb/erx084>.

Frank, G., Pressman, E., Ophir, R., Althan, L., Shaked, R., Freedman, M., et al., 2009. Transcriptional profiling of maturing tomato (*Solanum lycopersicum* L.) microspores reveals the involvement of heat shock proteins, ROS scavengers, hormones, and sugars in the heat stress response. *J. Exp. Bot.* 60, 3891–3908. <https://doi.org/10.1093/jxb/erp234>.

Fu, J.J., Miao, Y.J., Shao, L.H., Hu, T.M., Yang, P.Z., 2016. De novo transcriptome sequencing and gene expression profiling of *Elymus nutans* under cold stress. *BMC Genomics* 17, 870. <https://doi.org/10.1186/s12864-016-3222-0>.

Garg, R., Singh, V.K., Rajkumar, M.S., Kumar, V., Jain, M., 2017. Global transcriptome and co-expression network analyses reveal cultivar-specific molecular signatures associated with seed development and seed size/weight determination in chickpea. *Plant J.* 91, 1088–1107. <https://doi.org/10.1111/tpj.13621>.

Gill, S.S., Tuteja, N., 2010. Reactive oxygen species and antioxidant machinery in abiotic stress tolerance in crop plants. *Plant Physiol. Biochem.* 48, 909–930. <https://doi.org/10.1016/j.plaphy.2010.08.016>.

Gohar, T., Payal, A., Murray, G., Anil, K., 2010. MAPK machinery in plants recognition and response to different stresses through multiple signal transduction pathways. *Plant Signal. Behav.* 5 (11), 1370–1378. <https://doi.org/10.4161/psb.5.11.13020>.

Grabherr, M.G., Haas, B.J., Yassour, M., Levin, J.Z., Thompson, D.A., Amit, I., et al., 2011. Full-length transcriptome assembly from RNA-Seq data without a reference genome. *Nat. Biotechnol.* 29, 644–652. <https://doi.org/10.1038/nbt.1883>.

Guan, Q., Yue, X., Zeng, H., Zhu, J., 2014. The protein phosphatase RCF2 and its interacting partner NAC019 are critical for heat stress-responsive gene regulation and thermotolerance in *arabidopsis*. *Plant Cell* 26, 438–453. <https://doi.org/10.1105/tpc.113.118927>.

Guo, M., Liu, J.H., Ma, X., Zhai, Y.F., Gong, Z.H., Lu, M.H., 2016. Genome-wide analysis of the Hsp70 family genes in pepper (*Capsicum annuum* L.) and functional identification of *CaHsp70-2* involvement in heat stress. *Plant Sci.* 252, 246–256. <https://doi.org/10.1016/j.plantsci.2016.07.001>.

Gupta, A.K., Kaur, N., 2005. Sugar signalling and gene expression in relation to carbohydrate metabolism under abiotic stresses in plants. *J. Biosci.* 30, 761–776. <https://doi.org/10.1007/BF02703574>.

Heckathorn, S.A., Downs, C.A., Sharkey, T.D., Coleman, J.S., 1998. The small, methionine-rich chloroplast heat-shock protein protects photosystem II electron transport during heat stress. *Plant Physiol.* 116, 439–444. <https://doi.org/10.1104/pp.116.1.439>.

Ifuku, K., Yamamoto, Y., Ono, T.A., Ishihara, S., Sato, F., 2005. PsbP protein, but not PsbQ protein, is essential for the regulation and stabilization of photosystem II in higher plants. *Plant Physiol.* 139, 1175–1184. <https://doi.org/10.1104/pp.105.068643>.

Ikeda, M., Mitsuda, N., Ohme-Takagi, M., 2011. Arabidopsis HsfB1 and HsfB2b act as repressors of the expression of heat-inducible Hsfs but positively regulate the acquired thermotolerance. *Plant Physiol.* 157, 1243–1254. <https://doi.org/10.1104/pp.111.179036>.

Iseli, C., Jongeneel, C.V., Bucher, P., 1999. ESTScan: a program for detecting, evaluating, and reconstructing potential coding regions in EST sequences. *Intell. Syst. Mol. Biol.* 138, 148.

Ivanov, A.G., Velitchkova, M.Y., Allakhverdiev, S.I., Huner, N.P.A., 2017. Heat stress-induced effects of photosystem I: an overview of structural and functional responses. *Photosynth. Res.* 133, 17–30. <https://doi.org/10.1007/s11120-017-0383-x>.

Jiang, C.G., Xu, J.Y., Zhang, H., Zhang, X., Shi, J.L., Li, M., et al., 2009. A cytosolic class I small heat shock protein, RchSP17.8, of *Rosa chinensis* confers resistance to a variety of stresses to *Escherichia coli*, yeast and *Arabidopsis thaliana*. *Plant Cell Environ.* 32, 1046–1059. <https://doi.org/10.1111/j.1365-3040.2009.01987.x>.

Jung, K.H., Ko, H.J., Nguyen, M.X., Kim, S.R., Ronald, P., An, G., 2012. Genome-wide identification and analysis of early heat stress responsive genes in rice. *J. Plant Biol.* 55, 458–468. <https://doi.org/10.1007/s12374-012-0271-z>.

Koskull-döring, P.V., Scharf, K.D., Nover, L., 2007. The diversity of plant heat stress

- transcription factors. *Trends Plant Sci.* 12, 452–457. <https://doi.org/10.1016/j.tplants.2007.08.014>.
- Koskull-Döring, P.V., Scharf, K., Nover, L., 2007b. The diversity of plant heat stress transcription factors. *Trends Plant Sci.* 12, 452–457. <https://doi.org/10.1016/j.tplants.2007.08.014>.
- Kotak, S., Larkindale, J., Lee, U., von Koskull-Döring, P., Vierling, E., Scharf, K.D., 2007. Complexity of the heat stress response in plants. *Curr. Opin. Plant Biol.* 10, 310–316. <https://doi.org/10.1016/j.cpb.2007.04.011>.
- Kovtun, Y., Chiu, W.L., Tena, G., Sheen, J., 2000. Functional analysis of oxidative stress-activated mitogen-activated protein kinase cascade in plants. *Proc. Natl. Acad. Sci. U.S.A.* 97, 2940–2945. <https://doi.org/10.1073/pnas.97.6.2940>.
- Kurek, I., Chang, T.K., Bertain, S.M., Madrigal, A., Liu, L., Lassner, M.W., et al., 2007. Enhanced Thermostability of Arabidopsis Rubisco activase improves photosynthesis and growth rates under moderate heat stress. *Plant Cell* 19, 3230–3241. <https://doi.org/10.1105/tpc.107.054171>.
- Langfelder, P., Horvath, S., 2008. WGCNA: an R package for weighted correlation network analysis. *BMC Bioinform.* 9, 559. <https://doi.org/10.1186/1471-2105-9-559>.
- Larkindale, J., Knight, M.R., 2002. Protection against heat stress-induced oxidative damage in Arabidopsis involves calcium, abscisic acid, ethylene, and salicylic acid. *Plant Physiol.* 128, 682–695. <https://doi.org/10.1104/pp.010320>.
- Larkindale, J., Hall, J.D., Knight, M.R., Vierling, E., 2005. Heat stress phenotypes of Arabidopsis mutants implicate multiple signaling pathways in the acquisition of thermotolerance. *Plant Physiol.* 138, 882–897. <https://doi.org/10.1104/pp.105.062257>.
- Lee, G.J., Vierling, E., 2000. A small heat shock protein cooperates with heat shock protein 70 systems to reactivate a heat-denatured protein. *Plant Physiol.* 122, 189–197. <https://doi.org/10.1104/pp.122.1.189>.
- Lee, U., Wie, C., Escobar, M., Williams, B., Hong, S.W., Vierling, E., 2005. Genetic analysis reveals domain interactions of Arabidopsis Hsp100/ClpB and cooperation with the small heat shock protein chaperone system. *Plant Cell* 17, 559–571. <https://doi.org/10.1105/tpc.104.027540>.
- Lee, U., Rioflorida, I., Hong, S.W., Larkindale, J., Waters, E.R., Vierling, E., 2007. The Arabidopsis ClpB/Hsp100 family of proteins: chaperones for stress and chloroplast development. *Plant J.* 49, 115–127. <https://doi.org/10.1111/j.1365-313X.2006.02940.x>.
- Li, X., Li, X., Li, M., Yan, Y., Liu, X., Li, L., 2016. Dual function of NAC072 in ABF3-mediated ABA-responsive gene regulation in arabidopsis. *Front. Plant Sci.* 7, 1075. <https://doi.org/10.3389/fpls.2016.01075>.
- Lim, C.J., Hwang, J.E., Chen, H., Hong, J.K., Yang, K.A., Choi, M.S., et al., 2007. Over-expression of the Arabidopsis DRE/CRT-binding transcription factor DREB2C enhances thermotolerance. *Biochem. Biophys. Res. Commun.* 362, 431–436. <https://doi.org/10.1016/j.bbrc.2007.08.007>.
- Liu, G.T., Wang, J.F., Cramer, G., Dai, Z.W., Duan, W., Xu, H.G., et al., 2012. Transcriptomic analysis of grape (*Vitisvinifera* L.) leaves during and after recovery from heat stress. *BMC Plant Biol.* 12, 174. <https://doi.org/10.1186/1471-2229-12-174>.
- Long, T.A., Okegawa, Y., Shikanai, T., Schmidt, G.W., Covert, S.F., 2008. Conserved role of proton gradient regulation 5 in the regulation of PSI cyclic electron transport. *Planta* 228, 907–918. <https://doi.org/10.1007/s00425-008-0789-y>.
- Luan, S., 2009. The CBL-CIPK network in plant calcium signaling. *Trends Plant Sci.* 14, 37–42. <https://doi.org/10.1016/j.tplants.2008.10.005>.
- Mangelsen, E., Kilian, J., Harter, K., Jansson, C., Wanke, D., Sundberg, E., 2011. Transcriptomic analysis of high-temperature stress in developing barley caryopses: early stress responses and effects on storage compound biosynthesis. *Mol. Plant* 4, 97–115. <https://doi.org/10.1093/mp/ssq058>.
- Meiri, D., Breiman, A., 2009. Arabidopsis ROF1 (FKBP62) modulates thermotolerance by interacting with HSP90.1 and affecting the accumulation of HsfA2-regulated sHSPs. *Plant J.* 59, 387–399. <https://doi.org/10.1111/j.1365-313X.2009.03878.x>.
- Miller, G., Shulaev, V., Mittler, R., 2008. Reactive oxygen signaling and abiotic stress. *Physiol. Plantarum* 133, 481–489. <https://doi.org/10.1111/j.1399-3054.2008.01090.x>.
- Mittler, R., Vanderauwera, S., Gollery, M., Van Breusegem, F., 2004. The reactive oxygen gene network in plants. *Trends Plant Sci.* 9, 490–498. <https://doi.org/10.1016/j.tplants.2004.08.009>.
- Mulaudzi-Masuku, T., Mutepe, R.D., Mukhoro, O.C., Faro, A., Ndimba, B., 2015. Identification and characterization of a heat-inducible Hsp70 gene from *Sorghum bicolor* which confers tolerance to thermal stress. *Cell Stress Chaperones* 20, 793–804. <https://doi.org/10.1007/s12192-015-0591-2>.
- Munekage, Y., Hojo, M., Meurer, J., Endo, T., Tasaka, M., Shikanai, T., 2002. PGR5 is involved in cyclic electron flow around photosystem I and is essential for photo-protection in Arabidopsis. *Cell* 110, 361–371. [https://doi.org/10.1016/S0092-8674\(02\)00867-X](https://doi.org/10.1016/S0092-8674(02)00867-X).
- Muñoz, F.J., Barojafernández, E., Moránzorzano, M.T., Alonsocasajús, N., Pozuetaaromero, J., 2006. Cloning, expression and characterization of a nudix hydrolase that catalyzes the hydrolytic breakdown of adp-glucose linked to starch biosynthesis in arabidopsis thaliana. *Plant Cell Physiol.* 47, 926–934. <https://doi.org/10.1093/pcp/pcj065>.
- Nagamangala, K.C., Muroi, A., Maffei, M.E., Yoshioka, H., Sawasaki, T., Arimura, G.I., 2010. Ca<sup>2+</sup>-dependent protein kinases and their substrate HsfB2a are differentially involved in the heat response signaling pathway in Arabidopsis. *Plant Biotechnol.* 27, 469–473. <https://doi.org/10.5511/plantbiotechnology.10.0728b>.
- Nishizawa, A., Yabuta, Y., Shigeoka, S., 2008. Galactinol and raffinose constitute a novel function to protect plants from oxidative damage. *Plant Physiol.* 147, 1251–1263. <https://doi.org/10.1104/pp.108.122465>.
- Ohama, N., Kusakabe, K., Mizoi, J., Zhao, H., Kidokoro, S., Koizumi, S., et al., 2016. The transcriptional cascade in the heat stress response of arabidopsis is strictly regulated at the level of transcription factor expression. *Plant Cell* 28, 181–201. <https://doi.org/10.1105/tpc.15.00435>.
- Ohama, N., Sato, H., Shinozaki, K., Yamaguchi-Shinozaki, K., 2017. Transcriptional regulatory network of plant heat stress response. *Trends Plant Sci.* 22, 53–65. <https://doi.org/10.1016/j.tplants.2016.08.015>.
- Paredes, M., Quiles, M.J., 2012. Stimulation of chlororespiration by drought under heat and high illumination in *Rosa meilandina*. *J. Plant Physiol.* 170, 165–171. <https://doi.org/10.1016/j.jplph.2012.09.010>.
- Pei, H., Ma, N., Tian, J., Luo, J., Chen, J., Li, J., et al., 2013. An NAC transcription factor controls ethylene-regulated cell expansion in flower petals. *Plant Physiol.* 163, 775–791. <https://doi.org/10.1104/pp.113.223388>.
- Perteira, G., Huang, X.Q., Liang, F., Antonescu, V., Sultana, R., Karamycheva, S., et al., 2003. TIGR Gene Indices clustering tools (TGICL): a software system for fast clustering of large EST datasets. *Bioinformatics* 19, 651–652. <https://doi.org/10.1093/bioinformatics/btg034>.
- Plöschinger, M., Schwenkert, S., Sydow, L.V., Schröder, W.P., Meurer, J., 2016. Functional update of the auxiliary proteins PsbW, PsbY, HCF136, PsbN, TerC and ALB3 in maintenance and assembly of PSII. *Front. Plant Sci.* 7, 413. <https://doi.org/10.3389/fpls.2016.00423>.
- Qin, D., Wu, H., Peng, H., Yao, Y., Ni, Z., Li, Z., et al., 2008. Heat stress-responsive transcriptome analysis in heat susceptible and tolerant wheat (*Triticum aestivum* L.) by using Wheat Genome Array. *BMC Genomics* 9, 432. <https://doi.org/10.1186/1471-2164-9-432>.
- Radchuk, V.V., Borisjuk, L., Sreenivasulu, N., Merx, K., Mock, H.P., Rolletschek, H., et al., 2009. Spatiotemporal profiling of starch biosynthesis and degradation in the developing barley grain. *Plant Physiol.* 150, 190–204. <https://doi.org/10.1104/pp.108.133520>.
- Raymond, O., Gouzy, J., Just, J., Badouin, H., Verdenaud, M., Lemainque, A., et al., 2018. The *Rosa* genome provides new insights into the domestication of modern roses. *Nat. Genet.* <https://doi.org/10.1038/s41588-018-0110-3>.
- Reddy, A.S., Ali, G.S., Celesnik, H., Day, L.S., 2011. Coping with stresses: roles of calcium and calcium/calmodulin-regulated gene expression. *Plant Cell* 23, 2010–2032. <https://doi.org/10.1105/tpc.111.084988>.
- Sanmiya, K., Suzuki, K., Egawa, Y., Shono, M., 2004. Mitochondrial small heat-shock protein enhances thermotolerance in tobacco plants. *FEBS Lett.* 557, 265–268. [https://doi.org/10.1016/S0014-5793\(03\)01494-7](https://doi.org/10.1016/S0014-5793(03)01494-7).
- Schrader, S.M., Wise, R.R., Wacholtz, W.F., Ort, D.R., Sharkey, T.D., 2004. Thylakoid membrane responses to moderately high leaf temperature in Pima cotton. *Plant Cell Environ.* 27, 725–735. <https://doi.org/10.1111/j.1365-3040.2004.01172.x>.
- Shi, J., Yan, B., Lou, X., Ma, H., Ruan, S., 2017. Comparative transcriptome analysis reveals the transcriptional alterations in heat resistant and heat-sensitive sweet maize (*Zea mays* L.) varieties under heat stress. *BMC Plant Biol.* 17, 26. <https://doi.org/10.1186/s12870-017-0973-y>.
- Song, Y., Chen, Q., Ci, D., Shao, X.N., Zhang, D.Q., 2014. Effects of high temperature on photosynthesis and related gene expression in poplar. *BMC Plant Biol.* 14, 111. <https://doi.org/10.1186/1471-2229-14-111>.
- Su, P.H., Li, H.M., 2008. Arabidopsis stromal 70-kD heat shock proteins are essential for plant development and important for thermotolerance of germinating seeds. *Plant Physiol.* 146, 1231–1241. <https://doi.org/10.1104/pp.107.114496>.
- Sun, J., Ren, L.P., Cheng, Y., Gao, J.J., Dong, B., Chen, S.M., 2014. Identification of differentially expressed genes in *Chrysanthemum nankingense* (Asteraceae) under heat stress by RNA Seq. *Gene* 552, 59–66. <https://doi.org/10.1016/j.gene.2014.09.013>.
- Suzuki, N., Rizhsky, L., Hongjian, L., Shuman, J., Shulaev, V., Mittler, R., 2005. Enhanced tolerance to environmental stress in transgenic plants expressing the transcriptional coactivator multiprotein bridging factor 1c. *Plant Physiol.* 139, 1313–1322. <https://doi.org/10.1104/pp.105.070110>.
- Suzuki, N., Sejima, H., Tam, R., Schlauch, K., Mittler, R., 2011. Identification of the MBF1 heat-response regulon of Arabidopsis thaliana. *Plant J.* 66, 844–851. <https://doi.org/10.1111/j.1365-313X.2011.04550.x>.
- Taji, T., Ohsumi, C., Iuchi, S., Seki, M., Kasuga, M., Kobayashi, M., et al., 2010. Important roles of drought- and cold-inducible genes for galactinol synthase in stress tolerance in Arabidopsis thaliana. *Plant J.* 29, 417–426. <https://doi.org/10.1046/j.0960-7412.2001.01227.x>.
- Thoday-Kennedy, E.L., Jacobs, A.K., Roy, S.J., 2015. The role of the CBL-CIPK calcium signaling network in regulating ion transport in response to abiotic stress. *Plant Growth Regul.* 76, 3–12. <https://doi.org/10.1007/s10725-015-0034-1>.
- Vacca, R.A., de Pinto, M.C., Valenti, D., Passarella, S., Marra, E., De Gara, L., 2004. Production of reactive oxygen species, alteration of cytosolic ascorbate peroxidase, and impairment of mitochondrial metabolism are early events in heat shock-induced programmed cell death in tobacco Bright-Yellow 2 cells. *Plant Physiol.* 134, 1100–1112. <https://doi.org/10.1104/pp.103.035956>.
- Valmonte, G.R., Colleen, K.A., Robin, M.H., MacDiarmid, M., 2014. Calcium-dependent protein kinases in plants: evolution, expression and function. *Plant Cell Physiol.* 55, 551–569. <https://doi.org/10.1093/pcp/pct200>.
- Wan, X.L., Zhou, Q., Wang, Y.Y., Wang, W.E., Bao, M.Z., Zhang, J.W., 2015. Identification of heat-responsive genes in carnation (*Dianthus caryophyllus* L.) by RNA-seq. *Front. Plant Sci.* 6, 519. <https://doi.org/10.3389/fpls.2015.00519>.
- Wang, J.M., Yang, Y., Liu, X.H., Huang, J., Wang, Q., Gu, J.H., et al., 2014. Transcriptome profiling of the cold response and signaling pathways in *Lilium lancifolium*. *BMC Genomics* 15, 203. <https://doi.org/10.1186/1471-2164-15-203>.
- Xing, W., Wang, Z., Wang, X., Bao, M., Ning, G., 2014. Over-expression of an FT homolog from *Prunus mume* reduces juvenile phase and induces early flowering in rugosa rose. *Sci. Hortic.* 172, 68–72. <https://doi.org/10.1016/j.scienta.2014.03.050>.
- Yan, J., Yu, L., Xuan, J.P., Lu, Y., Lu, S.J., Zhu, W.M., 2016. De novo transcriptome sequencing and gene expression profiling of spinach (*Spinacia oleracea* L.) leaves under heat stress. *Sci. Rep.* 6, 19473. <https://doi.org/10.1038/srep19473>.

- Ye, J., Fang, L., Zheng, H., Zhang, Y., Chen, J., Zhang, Z., et al., 2006. WEGO: a web tool for plotting GO annotations. *Nucleic Acids Res.* 34, W293–W297. <https://doi.org/10.1093/nar/gkl031>.
- Yoo, S.D., Cho, Y.H., Tena, G., Xiong, Y., Sheen, J., 2008. Dual control of nuclear EIN3 by bifurcate MAPK cascades in C2H4 signalling. *Nature* 451, 789–795. <https://doi.org/10.1038/nature06543>.
- Yu, Q., An, L., Li, W., 2014. The CBL–CIPK network mediates different signaling pathways in plants. *Plant Cell Rep.* 33, 203–214. <https://doi.org/10.1007/s00299-013-1507-1>.
- Zandalinas, S.I., Rivero, R.M., Martínez, V., Gómez-Cadenas, A., Arbona, V., 2016. Tolerance of citrus plants to the combination of high temperatures and drought is associated to the increase in transpiration modulated by a reduction in abscisic acid levels. *BMC Plant Biol.* 16, 105. <https://doi.org/10.1186/s12870-016-0791-7>.
- Zeng, Y.L., Tan, X.F., Zhang, L., Long, H.X., Wang, B.M., Li, Z., et al., 2015. A fructose-1,6-biphosphate aldolase gene from *Camellia oleifera*: molecular characterization and impact on salt stress tolerance. *Mol. Breed.* 35, 17. <https://doi.org/10.1007/s11032-015-0233-5>.
- Zhao, J., Sun, Z., Zheng, J., Guo, X.Y., Dong, Z.G., Huai, J.L., et al., 2009. Cloning and characterization of a novel CBL-interacting protein kinase from maize. *Plant Mol. Biol.* 69, 661–674. <https://doi.org/10.1007/s11103-008-9445-y>.
- Zhao, Y., Yu, W.G., Hu, X.Y., Shi, Y.H., Liu, Y., Zhong, Y.F., Wang, P., Deng, S.Y., Niu, J., Yu, X.D., 2018. Physiological and transcriptomic analysis revealed the involvement of crucial factors in heat stress response of *Rhododendron hainanense*. *Gene* 660, 109–110. <https://doi.org/10.1016/j.gene.2018.03.082>.
- Zou, J.J., Wei, F.J., Wang, C., Wu, J.J., Ratnasekera, D., Liu, W.X., et al., 2010. Arabidopsis calcium-dependent protein kinase CPK10 functions in abscisic acid- and  $Ca^{2+}$ -mediated stomatal regulation in response to drought stress. *Plant Physiol.* 154, 1232–1243. <https://doi.org/10.1104/pp.110.157545>.
- Zou, J.J., Li, X.D., Ratnasekera, D., Wang, C., Liu, W.X., Song, L.F., et al., 2015. Arabidopsis CALCIUM-DEPENDENT PROTEIN KINASE8 and CATALASE3 function in abscisic acid-mediated signaling and  $H_2O_2$  homeostasis in stomatal guard cells under drought stress. *Plant Cell* 27, 1445–1460. <https://doi.org/10.1105/tpc.15.00144>.